DOKUZ EYLÜL UNIVERSITY
GRADUATE SCHOOL OF NATURAL AND APPLIED SCIENCES

NUMERICAL AND EXPERIMENTAL INVESTIGATIONS OF THERMAL PERFORMANCE OF VENTILATION UNITS

by
Onur DEMİRBOLAT

February, 2022
İZMİR

NUMERICAL AND EXPERIMENTAL INVESTIGATIONS OF THERMAL PERFORMANCE OF VENTILATION UNITS

A Thesis Submitted to the
Graduate School of Natural and Applied Sciences of Dokuz Eylül University
In Partial Fulfillment of the Requirements for the Master of Science of
Department of Mechanical Engineering

by
Onur DEMİRBOLAT

February, 2022
İZMİR

M.Sc THESIS EXAMINATION RESULT FORM

We have read the thesis entitled **"NUMERICAL AND EXPERIMENTAL INVESTIGATIONS OF THERMAL PERFORMANCE OF VENTILATION UNITS "** completed by **ONUR DEMİRBOLAT** under supervision of **PROF.DR. DİLEK KUMLUTAŞ** and we certify that in our opinion it is fully adequate, in scope and in quality, as a thesis for the degree of Master of Science.

Prof. Dr. Dilek KUMLUTAŞ

Supervisor

Prof. Dr. Can Özgür ÇOLPAN

(Jury Member)

Asst. Prof. Dr. Özay AKDEMİR

(Jury Member)

Prof. Dr. Okan FISTIKOĞLU
Director
Graduate School of Natural and Applied Sciences

ACKNOWLEDGMENTS

I would like to thank to my supervisor Prof. Dr. Dilek KUMLUTAŞ who helped and supported me to make this study completed. I could not finish this thesis without her patience and mentorship during my Master of Science studies.

I would like to specially thank to M. Sc. Utku Alp YÜCEKAYA for his technical and personal supports.

I would like to express my gratitude to AERA Air Conditioning & Ventilation Technologies for using ANEMO Test Laboratory within the scope of this study and to İ. Mert SALMAN for his technical support and for each skill I learned from him.

Lastly, I would like to give my special thanks to my parents Filiz and Necmi DEMİRBOLAT and to my brother Emir DEMİRBOLAT for their trust and supports during all my education life.

Onur DEMİRBOLAT

NUMERICAL AND EXPERIMENTAL INVESTIGATIONS OF THERMAL PERFORMANCE OF VENTILATION UNITS

ABSTRACT

Today, it became a necessity providing clean air which provides the desired comfort conditions, to working and living spaces in buildings. Therefore, using ventilation and air conditioning devices increased throughout the world. To increase energy efficiency of these devices, components such as heat recovery exchanger, fan, filter and compressor used in the devices are being examined. As well as these components, thermal insulation performance of the casing which these components located is being examined.

In this study, experimental and numerical methods were followed. First, a prototype casing with a panel thickness of 50 mm was produced and an experiment was carried out according to requirements of EN 1886 standard. After the experimental study was completed, numerical study conducted. In numerical study, the numerical model with the same dimensions as tested prototype, was modeled by using computer software, and thermal analysis was made by using the commercial Computational Fluid Dynamics (CFD) software. After the numerical model was verified, the study was completed by creating and analyzing the numerical model of two sections with 55 and 60 mm panel thickness, and examining the effects of section thickness on thermal performance.

As a result of the study, panel thickness was increased from 50 mm to 55 mm, maximum temperature on the external surface of the casing decreased by approximately 10˚C. According to results, it was concluded that the optimum panel thickness is 55 mm, since the effect of the thermal performance that will be provided by increasing the section thickness is very small.

Keywords: Heat Recovery Device, CFD, EN 1886 Standard, HVAC

HAVALANDIRMA ÜNİTELERİNİN ISIL PERFORMANSININ SAYISAL VE DENEYSEL OLARAK İNCELENMESİ

ÖZ

Günümüzde, istenilen konfor şartlarını sağlayan temiz havanın, çalışma ve yaşam alanlarına sağlanması bir zorunluluk haline gelmiştir. Bu yüzden, Dünya genelinde havalandırma ve iklimlendirme cihazlarının kullanımı artmıştır. Bu cihazların enerji verimliliğini artırmak için cihazlarda kullanılan ısı geri kazanım eşanjörü, fan, filtre ve kompresör gibi komponentlerin verimliliğinin yanı sıra bu komponentlerin içinde bulunduğu kasanın ısı yalıtım performansı da incelenmektedir.

Bu çalışmada deneysel ve sayısal olmak üzere iki farklı yöntem izlenmiştir. Önce, 50 mm panel kalınlığına sahip bir prototip kasa üretilerek TS EN 1886 standardının gerekliliklerine göre deneysel sonuçlar elde edilmiştir. Sayısal çalışmada ise, deneyi yapılan prototiple aynı ölçülere sahip sayısal model bilgisayar ortamında modellenmiş ve ticari Hesaplamalı Akışkanlar Dinamiği (HAD) programı kullanılarak ısıl analizler yapılmıştır. Sayısal model doğrulandıktan sonra, çalışma 55 ve 60 mm panel kalınlığına sahip iki kesitin sayısal modeli oluşturulup analizleri yapılarak, kesit kalınlığının ısıl performansa etkileri incelenerek tamamlanmıştır.

Yapılan çalışma sonucunda, 50 mm olan panel kalınlığı 55 mm' ye artırıldığında kasa dış yüzeyinde okunan maksimum sıcaklık yaklaşık 10˚C azalmıştır. Elde edilen bulgulara göre, kesit kalınlığını daha fazla artırmanın sağlayacağı ısıl performansın etkisi çok küçük olduğundan, optimum panel kalınlığının 55 mm olduğu sonucuna varılmıştır.

Anahtar kelimeler: Isı Geri Kazanım Cihazı, HAD, EN 1886 Standardı, HVAC

CONTENTS

Page

M.Sc THESIS EXAMINATION RESULT FORM ii
ACKNOWLEDGMENTS iii
ABSTRACT iv
ÖZ v
LIST OF FIGURES ix
LIST OF TABLES xi

CHAPTER ONE - INTRODUCTION 1

1.1 Introduction 1
1.2 Literature 1
1.3 Aim and Motivation 13

CHAPTER TWO - HEATING VENTILATION AND AIR CONDITIONING SYSTEMS 14

2.1 Brief History of HVAC 14
2.2 Heating 15
2.3 Ventilation 15
2.3.1 Mechanical Ventilation 16
2.3.2 Natural Ventilation 17
2.4 Heat Recovery Ventilation 17
2.4.1 Recuperator Heat Recovery Exchangers 18
2.4.2 Regenerative Heat Recovery Exchangers 19
2.4.3 Run Around Coil Heat Recovery System 20
2.4.4 Heat Pipe Recovery System 21
2.5 Air Conditioning 22

CHAPTER THREE - EXPERIMENTAL STUDY 24

3.1 Anemo Test Laboratory 24
3.2 EN 1886 Standard 26
3.2.1 Thermal performance test 27
3.2.1.1 Thermal Transmittance 31
3.2.1.2 Thermal Bridging 32

CHAPTER FOUR - NUMERICAL STUDY 33

4.1 Computational Fluid Dynamics (CFD) 33
4.1.1 Introduction to CFD 33
4.1.2 The Fundamental equations of CFD 33
4.1.3 Conservation Laws 34
4.1.3.1 The Continuity Equation 34
4.1.3.2 The Momentum Equation 35
4.1.3.3 The Energy Equation 37
4.2 Numerical Study 39
4.2.1 CFD Model 39
4.2.2 Meshing 42
4.2.3 Boundary Conditions 44

CHAPTER FIVE - RESULTS AND DISCUSSIONS 46

5.1 Experimental Results 46
5.2 Numerical Results 48

CHAPTER SIX - CONCLUSIONS 52

REFERENCES.....53

LIST OF FIGURES

Page

Figure 1.1 Schematic of reverse heat leakage test method on refrigerator 4

Figure 1.2 Electrical heaters and thermocouples locations of the rest rig 5

Figure 1.3 Ventilation unit with cross – flow pcm heat exchanger 6

Figure 1.4 New AHU layout design with two heat exchangers 7

Figure 1.5 a) Heat flow and temperature sensor locations b) Numerical study result of the window section c) Temperature distribution of the envelope surface. 9

Figure 1.6 a) Composite material b) Material specimen 10

Figure 1.7 Scheme of test rig 11

Figure 1.8 Schematic of the problem 12

Figure 2.1 Hiearchy of ventilation systems 16

Figure 2.2 Heat recovery unit with for residential buildings 18

Figure 2.3 Recuperative type heat exchanger 19

Figure 2.4 Heat recovery system with rotating regenerator 20

Figure 2.5 Heat recovery system with run around coil 21

Figure 2.6 Heat recovery system with heat pipes 22

Figure 3.1 View of Anemo test laboratory 24

Figure 3.2 Outline drawing of Anemo test laboratory 25

Figure 3.3 Keysight 34970A data logger unit 26

Figure 3.4 Parts of mechanical performance 27

Figure 3.5 Installation of temperature sensors 28

Figure 3.6 Front view of experimental setup 29

Figure 3.7 Back view of experimental setup 29

Figure 3.8 Location of fans and heating elements inside of the experimental setup . 30

Figure 4.1 Schematic of control volume 34

Figure 4.2 Forces have an impact on minimum surface dS 37
Figure 4.3 External dimensions of prototype 40
Figure 4.4 Internal dimensions of prototype 40
Figure 4.5 View of panel section 41
Figure 4.6 Maximum top surface temperature for more number of elements 43
Figure 4.7 Average top surface temperature for more number of elements 43
Figure 4.8 Mesh structure of cfd model 44
Figure 5.1 Location of the maximum surface temperature 46
Figure 5.2 Front side temperature measuring results 47
Figure 5.3 Top surface temperature measuring results 47
Figure 5.4 Numerical study results of front view 48
Figure 5.5 Numerical study results of top view 49
Figure 5.6 Temperature measuring results of top view of 55 mm panel thickness model 50
Figure 5.7 Temperature measuring results of top view of 60 mm panel thickness model 51

LIST OF TABLES

Page

Table 3.1 Thermal transmittance classes 31

Table 3.2 Thermal bridging classes 32

Table 4.1 Dimensions of prototype 41

Table 4.2 Thermal conductivity of materials 42

Table 4.3 Node and element numbers 42

Table 4.4 Boundary conditions 44

Table 5.1 Experimental data 48

Table 5.2 Comparison of experimental and numerical results of front view 49

Table 5.3 Comparison of experimental and numerical results of top view 50

Table 5.4 Comparison of the temperature results of top view of models 51

CHAPTER ONE
INTRODUCTION

1.1 Introduction

Heating, ventilation, and air conditioning (HVAC) systems are used for maintaining indoor air quality (IAQ) at the intended level. Air handling units (AHU) are part of HVAC systems that several processes can be done inside of the unit such as cooling, heating, humidifying, dehumidifying, filtering, and mixing of the air (ASHRAE Terminology, 2021).

Due to global warming and limited energy resources in the World, day by day Countries comply with new obligations about the consumption of energy. There are many kinds of International Standards or Directives about saving and more efficient use of energy. EcoDesign Directives is the most comprehensive regulation for energy using products in European Union Countries (Directive 2005/32/EC, 2005).

1.2 Literature

There are many different types of studies about the increasing performance of AHU's in the literature. Most studies focused on a single component such as a heat exchanger, filter, or fan which take part in the enclosure of AHU. There are also studies examining the efficiency of ventilation units as a whole.

Navarro & Gomez (2005) developed a new mathematical method to calculate the thermal performance of cross - flow heat exchangers. They validated the methodology with analytical and theoretical study results from different researches. Comparison results showed that there are small errors between the mathematical method and other study results.

Söylemez (2007) proposed a mathematical formulation to find the optimum length of finned pipe for maximizing the efficiency of waste heat recovery system. Also, some economical properties can be calculated such as net life cycle energy savings or payback period of heat recovery system by using equations proposed in this study.

Liu, Claridge & Deng (2003) developed an air filter pressure drop model to calculate fan energy in AHU and verified with experimental data. Airflow rate, total using time, initial and final pressure drop at the nominal air flow rate are inputs for the model.

Blasinski, Rubina, Rubinova & Juza (2021) developed a mathematical model for operating a fan rely on carbon dioxide concentration of the indoor air in an HVAC system. They examined 7 fan control algorithm variants and as the results compared, up to 65% energy can be saved with decreasing total fan operating time.

Kwon et al. (2011) designed an air filtration device by using commercial computational fluid dynamics software. They suggested using two axial-flow cyclones instead of air filter in AHU. They also conducted an experimental study and calculated particle collection efficiency and pressure drop.

Tian & Mo (2019) designed a novel electrostatically assisted air (EAA) filter structure and experimentally evaluated some parameters for optimizing filter efficiency. They compared EAA filters with commercial filters, found that EAA filters have better filtration performance and consume less energy.

Beşer, Mobedi & Kumlutaş (2001) studied the thermal performance of AHU casings by using commercial computational fluid dynamics software and thermograph method. They defined ideal casing in terms of thermal performance as homogeneous temperature distribution on the casing surface.

Korkmaz (2013) investigated the performance of heat recovery exchanger experimentally, numerically, and theoretically. Numerical results verified with experimental results. By using the numerical method with same boundary conditions, were optimized heat recovery exchanger dimensions.

Zenginoğlu, Koçak & Salman (2019) searched for a new air handling unit casing design that has better thermal insulation performance by using numerical and experimental methods. They obtained specific thermal bridging points on the casing and developed more efficient casing designs.

According to the literature, all components are investigated and developed individually such as heat exchangers, fans, and air filters in terms of energy efficiency. However, there are not enough studies about the casing where components are placed inside of AHU. Due to lack of study on this specific area in literature, studies conducted for similar purpose were examined.

Thiessen, Knabben, Melo & Gonçalves (2018) studied effects of vacuum insulation panels (VIP) on refrigerator insulation performance. They developed prototypes with different VIP configurations and did experiments using heat leakage test method. Experiment method schematic is shown in Figure 1.1. The results showed that covering 51% of the enclosure area with VIP, cause 21% decrease in energy consumption.

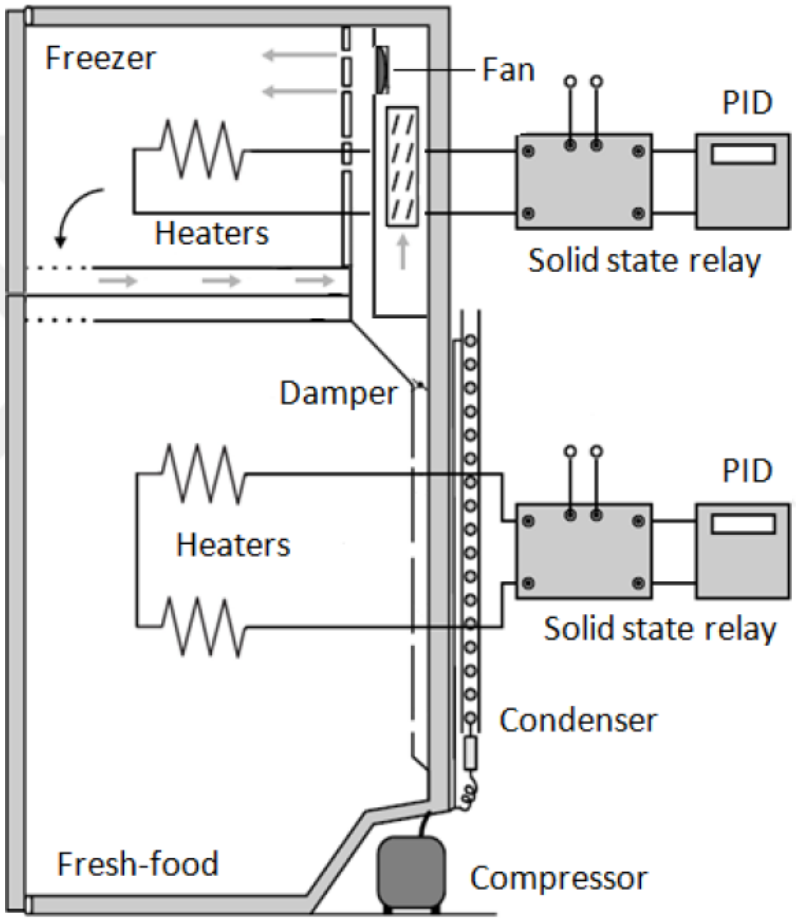


Figure 1.1 Schematic of reverse heat leakage test method on refrigerator (Thiessen, Knabben, Melo & Gonçalves, 2018)

Gulmez & Yilmaz (2020) studied heat transfer performance of refrigerator door gasket to eliminate condensation on the gasket surface by using experimental and numerical methods. The main purpose of the study is to increase temperature on the gasket surface where condensation occurs. They did experiments using reverse heat leakage method as seen in Figure 1.2. Electrical heaters were placed inner sections of the refrigerator to increase and keep stable temperature of inside air. Also, test chamber air temperature can be kept at desired value. Set values of air temperatures of inner and outer of the refrigerator are, 40 ˚C and 16 ˚C respectively. After the system reached steady state, the power supplied to electrical heaters is used for calculating overall thermal conductance of refrigerator casing. Same boundary conditions were used in the numerical model and they validated numerical model results with experimental data. A new gasket design was used in same model and according to the results temperature increased on the gasket surface by about 7%.

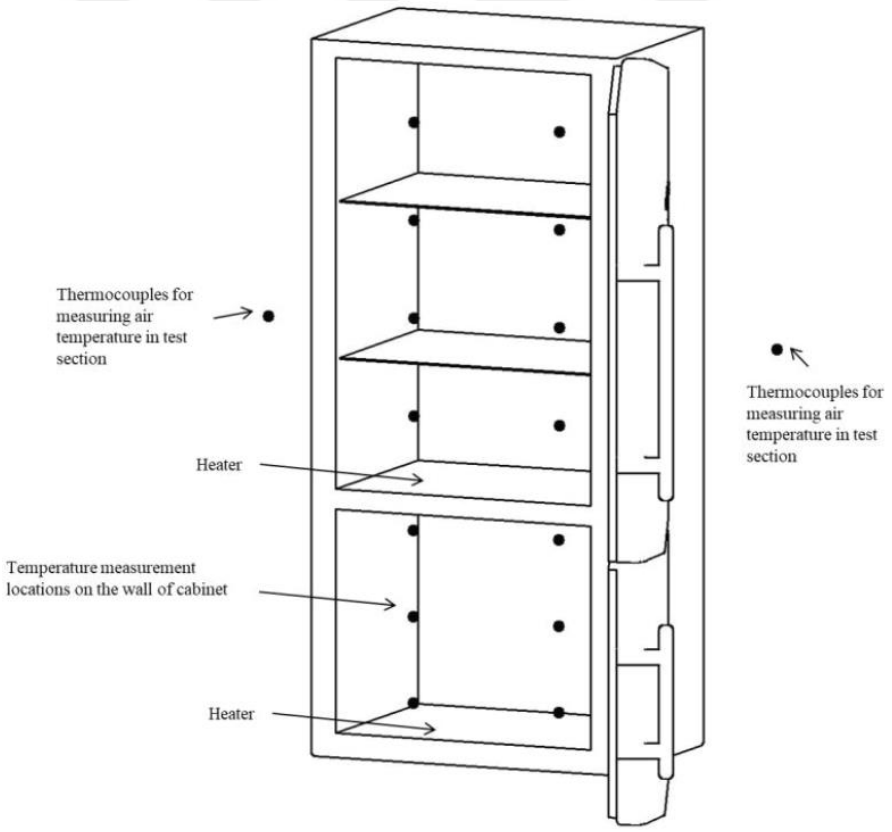


Figure 1.2 Electrical heaters and thermocouples locations of the rest rig (Gulmez & Yilmaz, 2020)

Promoppatum, Yao, Hultz & Agee (2017) conducted an experimental and numerical study on the thermal performance of ventilation units with phase change material (PCM) based cross-flow heat exchanger. A schematic of the ventilation system is shown in Figure 1.3. Heat exchangers were placed in two air ducts. Internal air pass through the heat exchanger and its energy is accumulated on pcm heat exchanger. By using flap and splitter fresh air pass through the heat exchanger, thus cold environment air gets warmer. With using two heat exchangers, this process keeps going so that continuous ventilation can be provided.

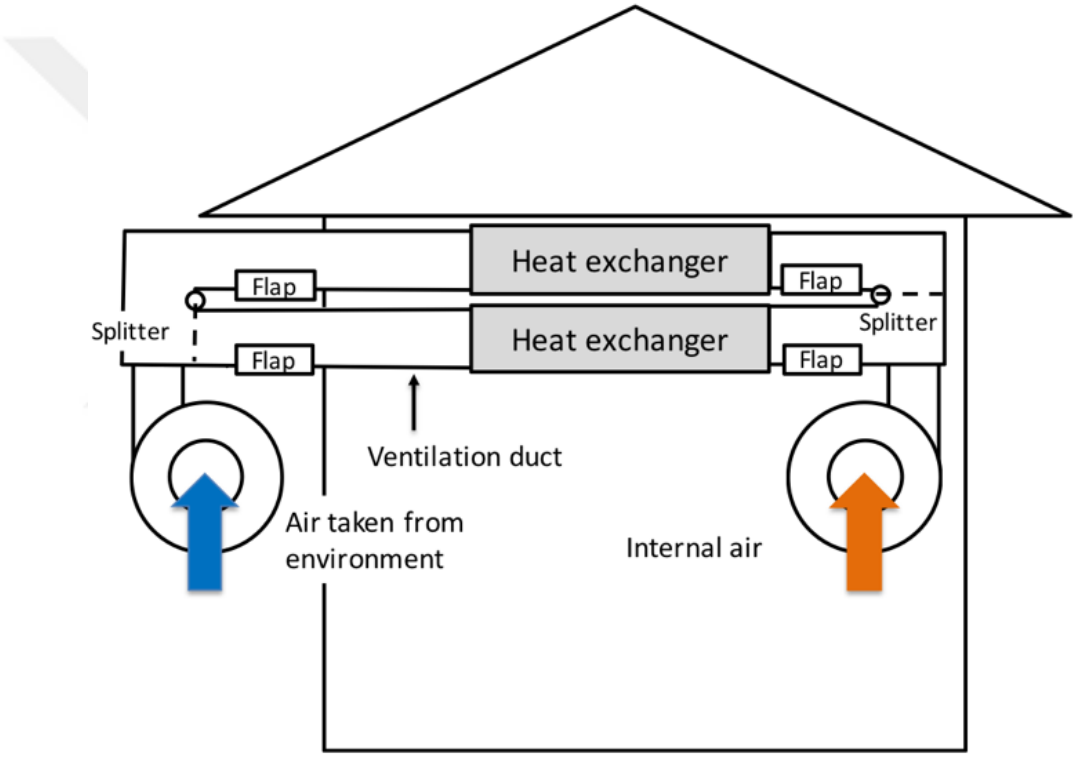


Figure 1.3 Ventilation unit with cross – flow pcm heat exchanger (Promoppatum, Yao, Hultz & Agee, 2017)

Some parameters were investigated numerically such as operational time, numbers of tube rows, tube diameter, and results validated with experiments. Also, different PCM's with various melting temperatures were examined.

Kalbashi, Shahsavar & Afrand (2019) proposed a new layout design using two heat recovery units for an AHU. As seen in Figure 1.4 secondary heat exchanger was placed downstream of the cooling coil. Energy consumption was calculated according to first law of thermodynamics for common and new layout of AHU, under summer weather conditions. For the common layout, at relative humidity of 10% and 80%, increasing of 10 ˚C of outdoor air temperature, energy consumption became more 12.62% and 30.86% respectively. On the other hand with new layout design, the increase in energy consumption became 2.48% and 29.73% respectively. The results showed that using new layout design made less energy consumption up to 26.38% less for hot and dry climates.

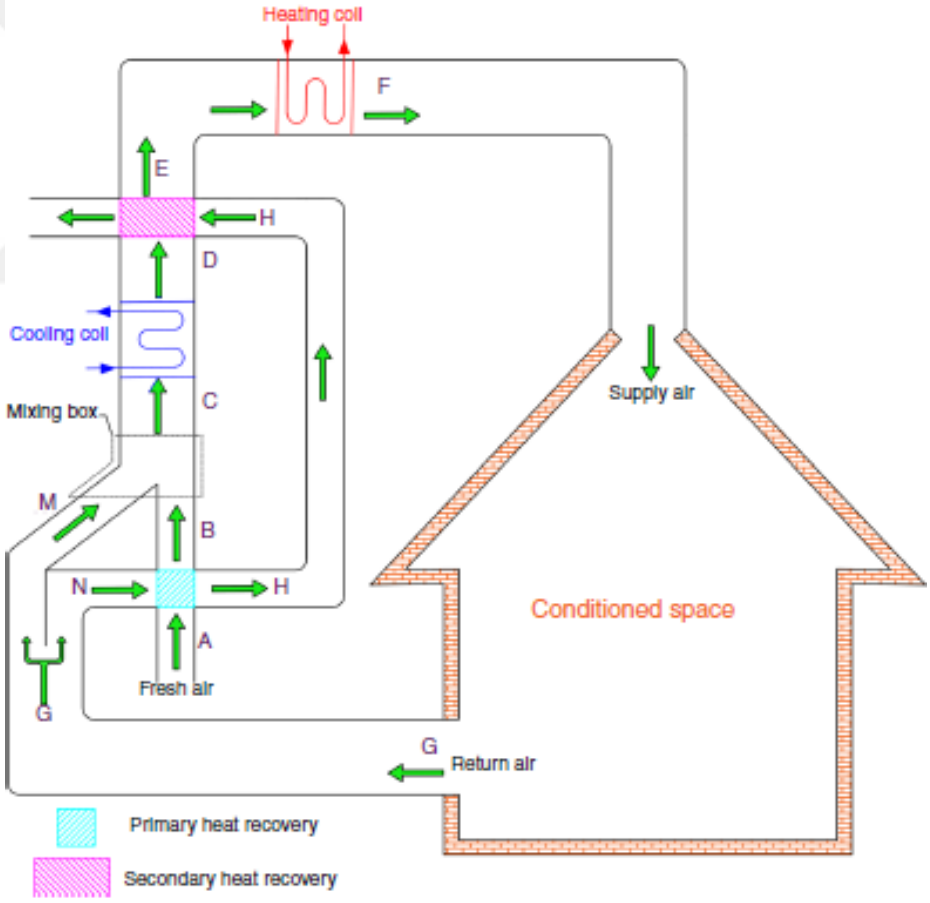


Figure 1.4 New AHU layout design with two heat exchangers (Kalbashi, Shahsavar & Afrand, 2019)

Baba & Ge (2016) investigated thermal bridging effects of balconies on energy performance of residential buildings. They used equivalent U - value method and commercial engineering software WUFI Plus to obtain thermal bridges on the buildings. Results showed that using thermal breaks in the balcony junctions reduces about 8 % of the annual heating load. If both sides of the walls above and below the balcony, up to 21.7% of energy can be saved.

Asdrubali, Baldinelli & Bianchi (2011) proposed a quantitative approach that can be used to describe thermal bridges on the surface of a part of the building envelopes. They used thermography method to identify temperature distribution experimentally. Also, temperature and heat flow sensors were placed to visualize temperature distribution of the surface, and results were validated with thermographic image of the envelope surface. Following studies were conducted analytically and numerically. Numerical model was prepared according to standard EN ISO 10077-2. Winter weather conditions were examined which is the inner side of the envelope warmer than the outer side. The sample was placed between two rooms and temperature difference of the room airs were kept at 20 ˚C in steady state. Same boundary conditions were used in numerical study.

In Figure 1.5 following features can be seen: locations of the heat flux and temperature sensors from the inner view(a), numerical study result of the window section (b), temperature distribution of the surface of the envelope from the inner view by thermography method (c). The scale of D on image (c) shows that minimum and maximum temperatures are 11.4 and 17.9 ˚C, respectively. When the results of three methods were compared, temperatures on the window surface showed good agreement. By using same methods different envelopes were investigated and obtained thermal bridges within this study.

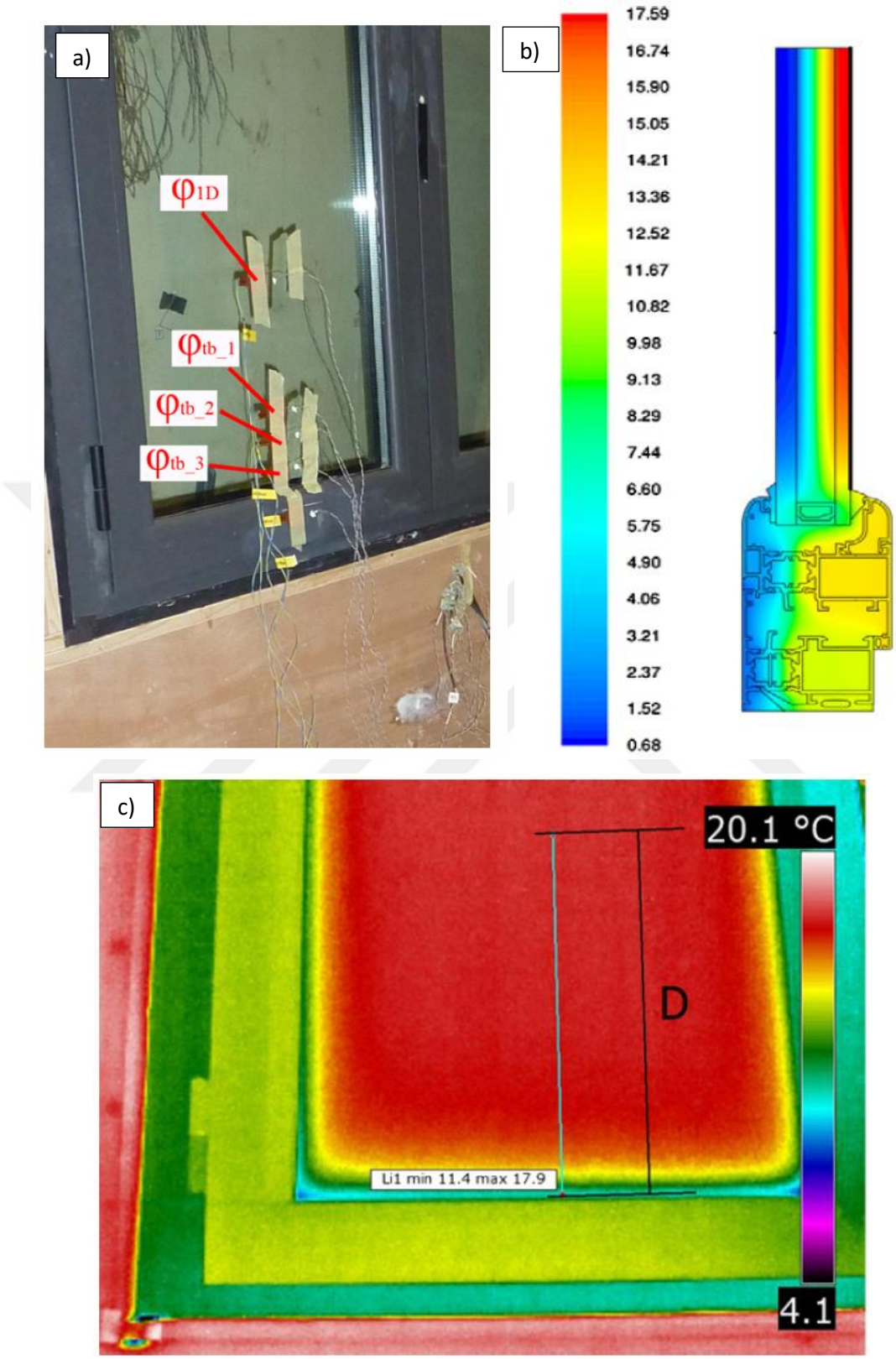


Figure 1.5 a) Heat flow and temperature sensor locations b) Numerical study result of the window section c) Temperature distribution of the envelope surface (Asdrubali, Baldinelli & Bianchi, 2011)

Pospisil, Pencik, Matejka, Kaluzova, & Dostalova, (2012) developed a new composite material that can be used as a thermal insulation element. Thus, thermal bridge effects on buildings envelopes can be eliminated and energy performance can be increased. In Figure 1.6 composite material which consists of binder and filler (a) and an example of material specimen (b) are shown.

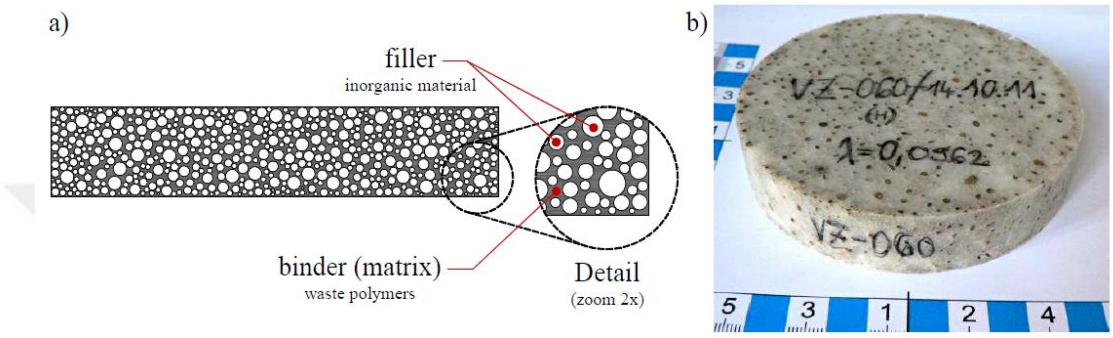


Figure 1.6 a) Composite material b) Material specimen (Pospisil, Pencik, Matejka, Kaluzova, & Dostalova, 2012)

Waste polymers like polypropylene (PP), polyethylene (PE), low density polyethylene (LDPE), and high density polyethylene (HDPE) can be used as a binder. To get minimum thermal conductivity λ [W/mK], PP (λ = 0.22 W/mK) was chosen as a binder. As a filler material LIAVER (λ = 0.06 – 0.07 W/mK) was used which has low thermal conductivity. To derive composite material which has good thermal insulation properties, possible maximum filler material, and minimum binder material were used. When these materials get together, new composite material has lower thermal conductivity (λ = 0.093 W/mK). New developed material can be used in places that need good thermal insulation and mechanical performance. In the second part of this study, decreasing of thermal losses was calculated according to CSN EN ISO 10211 Standard Thermal bridges in civil structures – thermal flows and surface temperatures – detailed calculations. Using new developed material, 6% energy can be saved in buildings.

Martin, Campos-Celador, Escudero, Gomez, & Sala, (2012) conducted a series of tests to obtain effects of thermal bridges in order to increase energy performance of buildings. They studied characteristics of a pillar thermal bridge and used commercial software FLUENT to compare simulation results with test results. The test rig consists of two air conditioning rooms which were used as hot and cold chambers as shown in Figure 1.7. Between two rooms test specimen were placed. To define thermal resistance value of the specimen, temperatures were set at 0 ˚C and 20 ˚C in cold and hot chambers, respectively. They calculated U value by using the power generated in hot chamber, surface area, and temperature difference between two rooms.

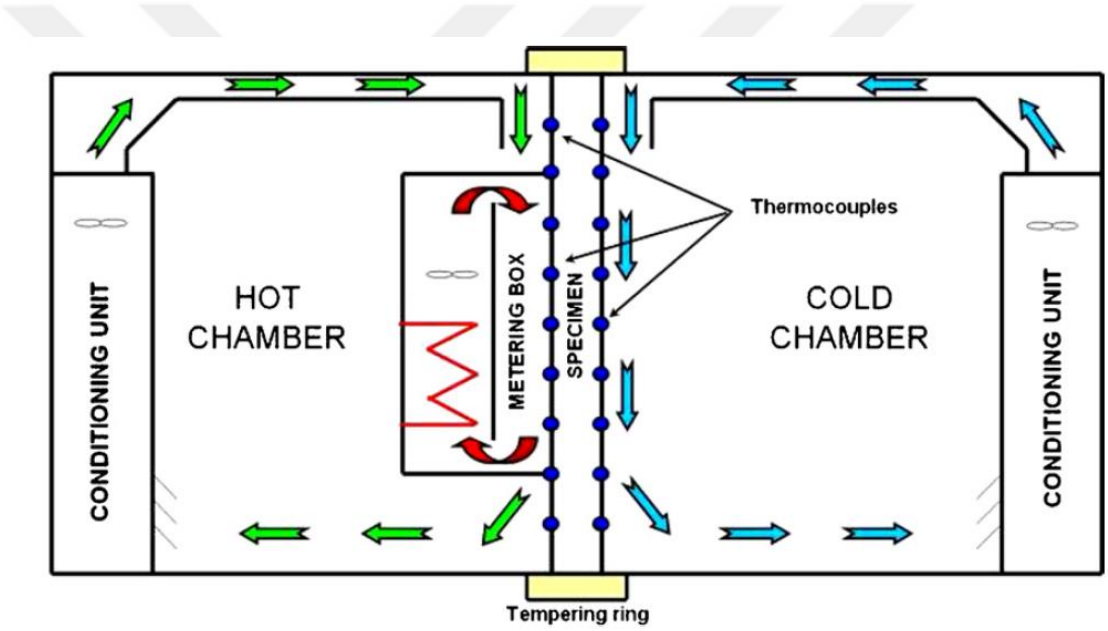


Figure 1.7 Scheme of test rig (Martin, Campos-Celador, Escudero, Gomez, & Sala, 2012)

To compare results of simulation and test, same boundary conditions were used in simulation tool. The results of tests conducted according to EN ISO 8990 Thermal insulation - determination of steady-state thermal transmission properties - calibrated and guarded hot box standard, compromising with the simulation results with 2% error margin.

Lei, Bortolin, Bison & Maldague (2017) conducted a numerical and experimental study to obtain thermal bridges on insulated truck box panels. They examined different types of defects that can be seen such as air gap, sawdust, steel dust, and water were filled into the polystyrene foam which is used as a main insulation material. They did experiments for hot and cool weather conditions. To measure temperature on the specimen active infrared thermography method was used. They also developed numerical method by using commercial software COMSOL Multiphysics. According to results, while the effects of water and steel dust were detectable, sawdust effect was ignorable.

Tadeu, Simoes, I., Simoes, N. & Prata (2011) studied thermal bridges on the buildings envelope which more realistic conditions for variable indoor and outdoor air temperatures per time. They used boundary element model (BEM) to solve the problem which can be seen in the schematic in Figure 1.8. Thus, by using the obtained time solutions can be used for any external temperature conditions. The BEM algorithm was validated with experimental results. Thermal conductivity was measured by the Guarded hot plate method.

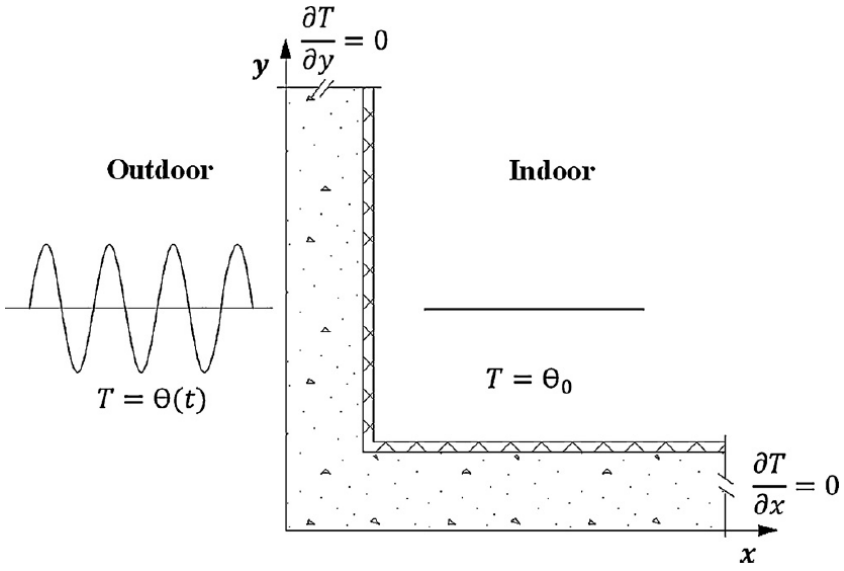


Figure 1.8 Schematic of the problem (Tadeu, Simoes, I., Simoes, N. & Prata 2011)

1.3 Aim and Motivation

The aim of this study is to design a new casing structure, more efficient in terms of heat transfer for an air handling unit by using computational fluid dynamics (CFD) software. Thus, better thermal bridging class will be obtained as stated in following chapters. Although many companies in HVAC industry indicated some studies on developing new casing structure, there is not clear investigation method in the literature due to commercial privacy and patents. New design of casing with better thermal insulation ensured that heat leakages were minimized and unintended condensation on the inner side of casing surface was prevented. Thus, more energy saving, and more healthy indoor air can be supplied for occupants in a building.

To make certain of the CFD Analysis results, an experimental study was conducted. Experimental study conducted according to EN 1886 “Ventilation for buildings - Air handling units - Mechanical performance” standard. After validating CFD results with the experimental results, new casing designs were studied. To improve insulation of the casing, effects of different parameters such as thickness of the materials, thermal conductivity of the materials, and profile sections were investigated.

CHAPTER TWO
HEATING VENTILATION AND AIR CONDITIONING SYSTEMS

2.1 Brief History of HVAC

Fire has been used to get warm spaces where people live since ancient times. To keep fire constant required fresh air supply and exhausting flue gas from indoor environment, ventilation needings arised. Many countries started to design and use ventilation systems by the end of the 19th century. Requirements to keep foods frozen cooling and ice making systems were invented. In 1902 New York Stock Exchange was cooled for the comfort of occupants. “Air conditioning” term was used for comfort cooling. However, heating, ventilation, and air conditioning (HVAC) term is used in general. Today’s modern HVAC technology was invented at the beginning of the 20th century with studies of Hermann Rietschel, Stuart Cramer, Willis Carrier, and many others. HVAC Industry includes controlling of these:

- Temperature
- Humidity
- Supplying fresh air
- Filtration of air
- Air transport in buildings

In modern times HVAC systems are used in many areas such as commercial and residential buildings, schools, hospitals, manufacturing processes, or for animal farms. For indoor places used by people, keeping indoor air quality (IAQ) at the intended level is the main purpose of HVAC (McDowall, 2006).

2.2 Heating

There are different types of heating buildings. Every type has advantages and disadvantages compared to each other, such as expensive initial investment cost, inefficient characteristics, or fuel type. Heating methods can be classified as follows:

- Heat transferring medium
- The fuel used
- Nature of heat
- Efficiency and desirability of the method

Heat transferring medium indicates what carries the heat from its main source to heated area. These mediums are air, water, steam, and electricity. Wood, coal, electricity, natural gas or fuel oil can be used as a fuel to produce heat (Brumbaugh, 2004).

Heating systems can also divide into two groups direct and indirect systems. Direct systems, the fuel to get heat is used or consumed in the area to be heated. Direct fire gas or oil heaters or electrical heaters can be given as an example for these systems. Heat transfer fluid is used by indirect systems to transfer the heat from fuel to be heated area. Following examples can be given for indirect systems: heat pumps and boilers.

2.3 Ventilation

Ventilation is an obligation for residential and commercial buildings. Clean and fresh air is supplied to the rooms where occupied by people through mechanical or natural ventilation methods.

There are three types of ventilation systems for non – domestic buildings: contingency, zoned, and complementary. Natural ventilation is used in contingency

type. However, mechanical ventilation can be adopted to the building when it is necessary. Different systems can be used for the different parts of the building, in zoned type. The complementary type allows to use of both systems, but systems can operate in different times. Hierarchy of ventilation systems are shown in Figure 2.1 (Etheridge, 2012).

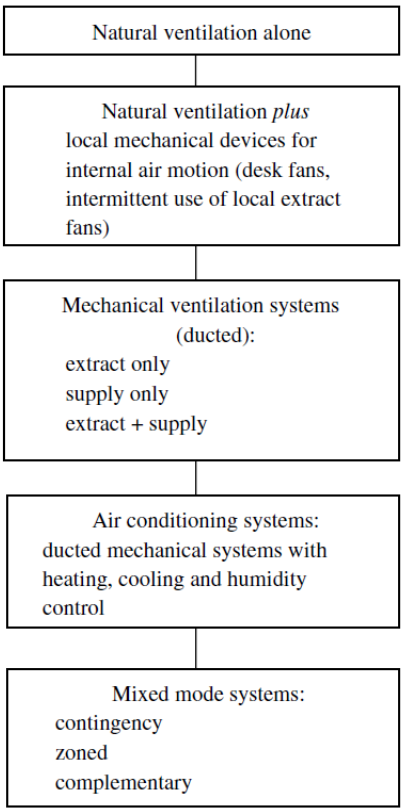


Figure 2.1 Hiearchy of ventilation systems (Etheridge, 2012)

2.3.1 Mechanical Ventilation

To supply fresh air to the buildings adequately, mechanical ventilation systems can be used which driven by fans. If natural ventilation is inadequate for maintaining indoor air quality, this ventilation method is used. Although maintaining enough indoor air quality, these systems do not efficient without heat recovery systems.

Because energy of the indoor air is discharged to outside with its energy. To use this waste energy heat recovery ventilation systems are used.

2.3.2 Natural Ventilation

Natural ventilation is driven by forces that take place due to temperature or pressure difference between indoor and outdoor air. There is no fan driven air circulation thus, this method of ventilation is energy free. Also, it has less initial investment cost compared to mechanical ventilation. Disadvantages of natural ventilation is not adequate for the buildings in very hot or cold climates. Air should be cooled or heated by a mechanical system. Also, controlling the indoor air quality is not possible in natural ventilation systems as much as in mechanical ventilation.

2.4 Heat Recovery Ventilation

To utilize energy of exhaust air comes from the buildings, heat recovery exchangers are used in mechanical ventilation systems. In HVAC systems up to 90% of waste heat can be recovered (Korkmaz, 2013). The process of transferring energy from exhaust air to fresh air can be done by using different types of heat exchangers. Heat recovery ventilator is shown in Figure 2.2.

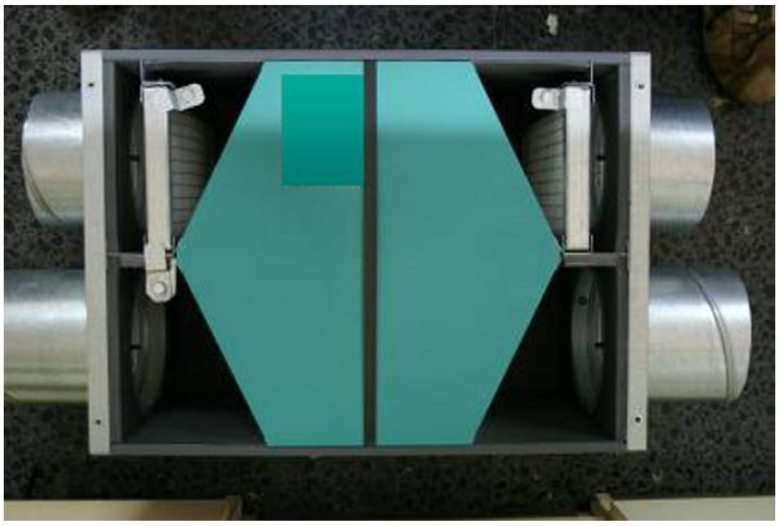


Figure 2.2 Heat recovery unit with for residential buildings (Seara, Diz, Uhia, Dopazo & Ferro, 2010)

2.4.1 Recuperator Heat Recovery Exchangers

In recuperator type heat exchangers, fluids are separated by a plate that conducts the heat from hot fluid to cold fluid. Fluid flows constantly and is never mixed. There is no movable part in the recuperator. The advantages of these types, simplicity in terms of manufacturability, rigid casing, and less thermal shock due to uniform temperature distribution. Disadvantages of these types are limits of temperature and pressure of the fluids (Thulukkanam, 2013). Recuperative type cross flow heat exchanger can be seen in Figure 2.3.

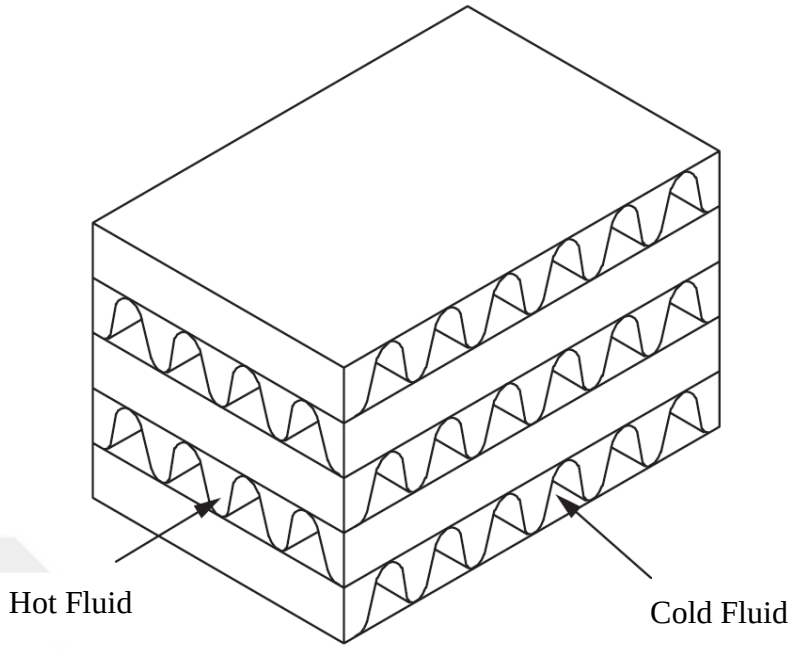


Figure 2.3 Recuperative type heat exchanger (Thulukkanam, 2013)

2.4.2 Regenerative Heat Recovery Exchangers

There is a medium which helps to transfer heat between hot and cold fluid. This flow process continues periodically and alternatively. In Figure 2.4, heat recovery schematic can be seen. At the beginning of the process, warm airflow through heat exchanger medium and its temperature raises. Then, cold air pass through the medium and its temperature raises. This process occurs while regenerator rotates.

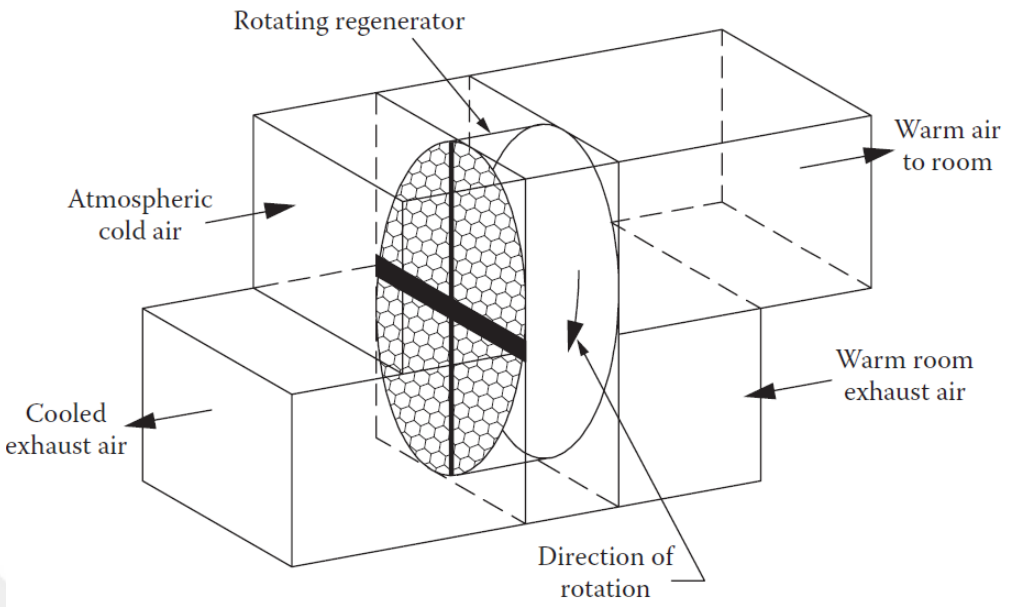


Figure 2.4 Heat recovery system with rotating regenerator (Thulukkanam, 2013)

2.4.3 Run Around Coil Heat Recovery System

In run around coil heat recovery systems, there are two heat exchangers that connected to each other via pipes which carry heat transfer fluid. Water is usually used as a fluid and circulates by using a circulating pump. Heat recovery process schematic with run around coil is shown in Figure 2.5. The process takes place as follows in winter climate conditions; waste heat is transferred from the exhaust hot air to fluid on exhaust heat exchanger and fresh cold air increases its energy by transferring on supply heat exchanger. Thus, supply air temperature will be increased before charging to the room. These types of heat recovery systems are usually used when hygienic conditions can be dangerous for human health. Because with this system air leakages or contaminant transfer from exhaust air side to supply air side due to lack of air tightening, is eliminated (Wallin, Madani & Claesson, 2012).

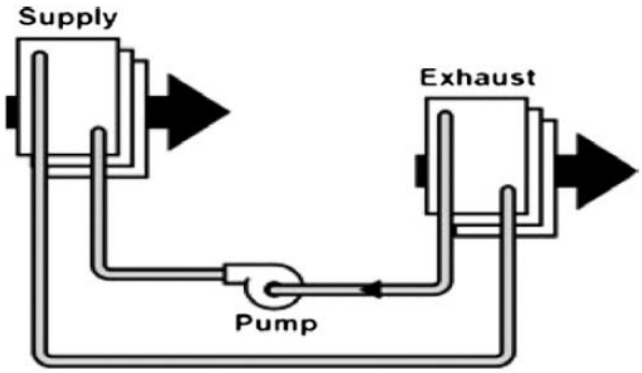


Figure 2.5 Heat recovery system with run around coil (Wallin, Madani & Claesson, 2012)

2.4.4 Heat Pipe Recovery System

Heat pipe heat exchangers have some advantages when compared to conventional ones. Heat transfer amount is larger when considering cross section area which makes more proper if there is not enough space for heat recovery unit. Other advantages are less pressure drop, cheap maintenance costs, and no need to mechanical drive for the liquid recirculation such as a pump. As shown in the Figure 2.6 evaporator section is placed bottom of the system to circulate condensed water inside of the pipes by using buoyancy force. Condensed water accumulates bottom of the system and water evaporates as the energy of hot exhausted gas to water which became gas. With gravity effect gas form of water pass through to upper side of the system.

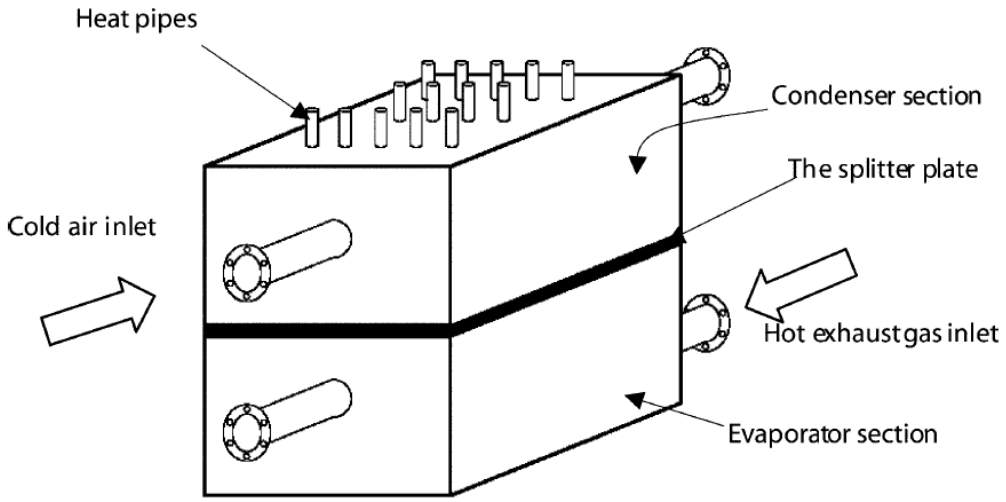


Figure 2.6 Heat recovery system with heat pipes (Yang, Yuan & Lin, 2003)

2.5 Air Conditioning

Air conditioning term is defined by American Society of Heating, Refrigeration, and Air Conditioning Engineers (2021) as, "the process of treating air to meet the requirements of a conditioned space by controlling its temperature, humidity, cleanliness and distribution." Process of treating air can be expressed as follows (Mcdowall, 2006):

- Heating
- Cooling
- Humidifying
- Dehumidifying
- Cleaning
- Ventilating
- Air Movement

All these processes or some of these can be used for treating air according to requirements. These requirements obtain from international standards and rules, health organizations, and climate conditions.

CHAPTER THREE
EXPERIMENTAL STUDY

3.1 Anemo Test Laboratory

Anemo test laboratory which is shown in Figure 3.1 meets the requirements of EN 17025, product development and validation can be done according to following standards: EN 308, EN 1886, EN 13053, and EN 13779.



Figure 3.1 View of Anemo test laboratory

Anemo test laboratory consists of two separate rooms as shown in Figure 3.2. 80 mm and 120 mm polyurethane insulation material (42 kg/m^3) is used in warm and cold room walls, respectively. With 20 kw heating capacity warm room air temperature can reach up to 37˚C and with 12 kw cooling capacity cold room air temperature can reach up to -25 ˚C.

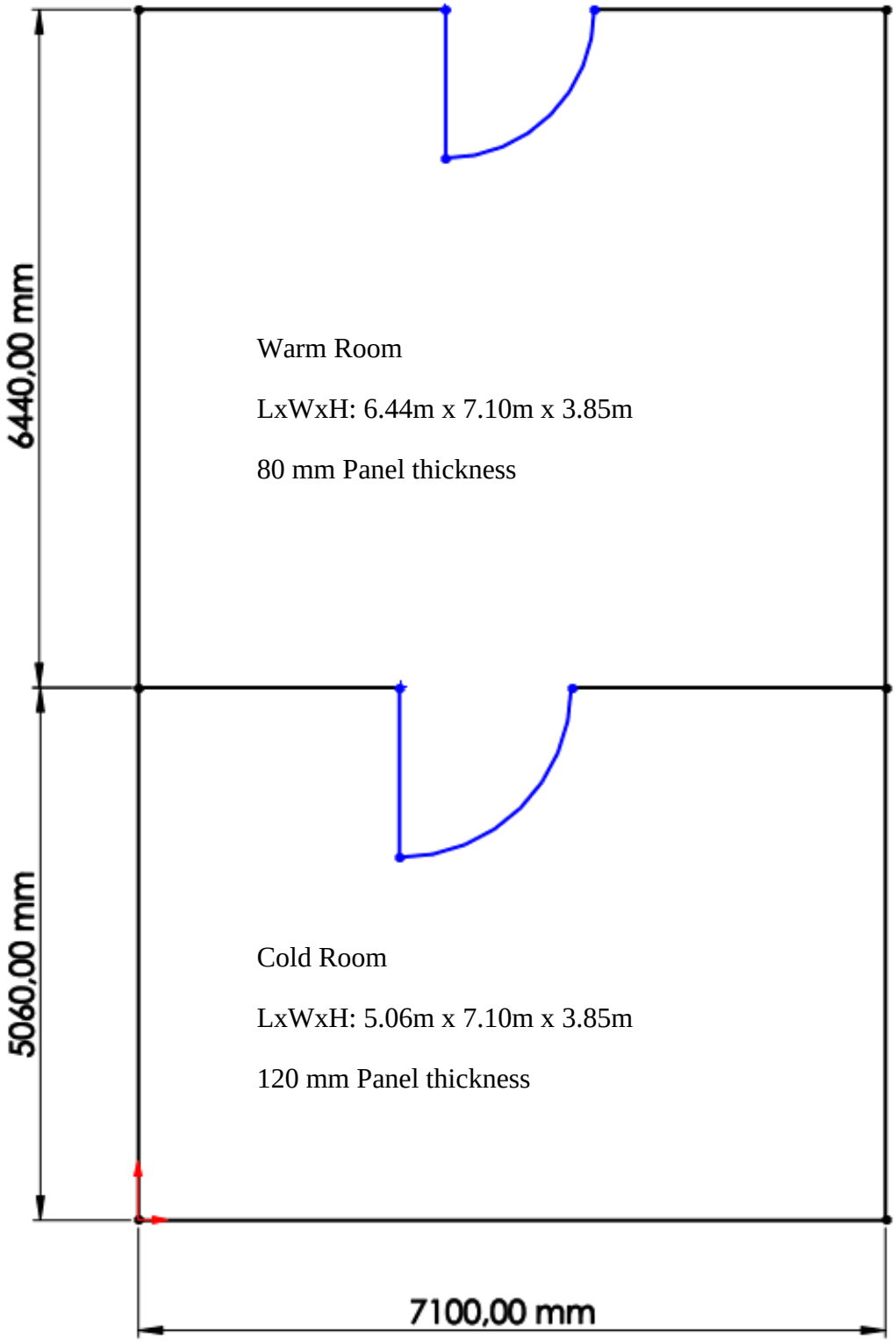


Figure 3.2 Outline drawing of Anemo test laboratory

Temperature measuring is performed by using 4 wire PT1000 temperature sensors and Keysight 34970A data acquisition system (Figure 3.3).



Figure 3.3 Keysight 34970A data logger unit

3.2 EN 1886 Standard

The content of this standard (EN 1886, 2007) is clarified in its foreword as follows; “The standard is a part of a series of standards for air handling units used for ventilation and air conditioning of buildings for human occupancy. It considers the mechanical performance of an air handling unit as a whole...” (p. 4).

Mechanical Performance of AHU was classified in EN 1886 “Ventilation for buildings - Air handling units - Mechanical performance” standard. Parts of mechanical performance can be seen in Figure 3.4.

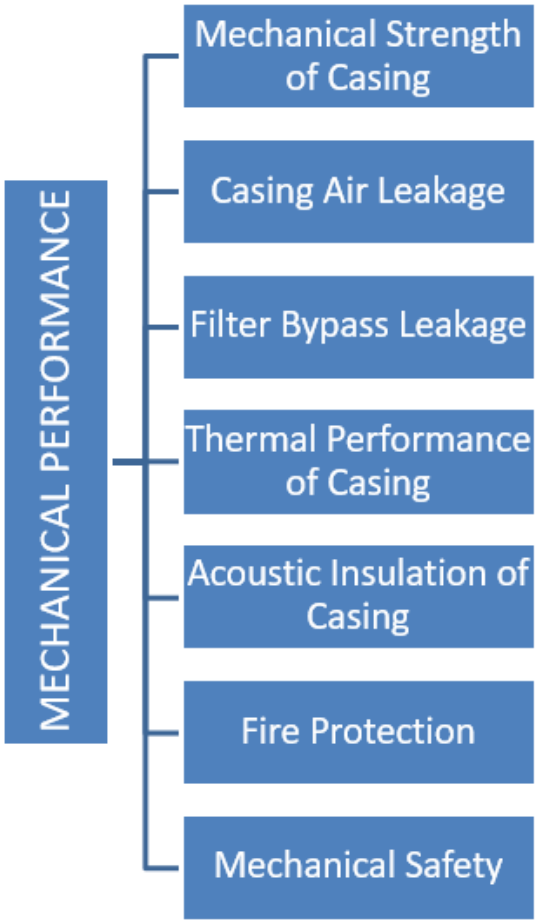


Figure 3.4 Parts of mechanical performance (EN 1886 Standard, 2007)

Within the scope of this study, Thermal performance of casing part was studied.

3.2.1 Thermal performance test

Casing consists of panels that have 50 mm thickness, were manufactured for the experimental study. The positions of temperature sensors should be located according to EN 1886 standard as shown in Figure 3.5. The front and back view of experimental setup, after temperature sensors are located, can be seen in Figure 3.6 and Figure 3.7.

The enclosure is divided to three equal zone. Externally controllable heaters and fans are located inside of the enclosure as shown in Figure 3.8.

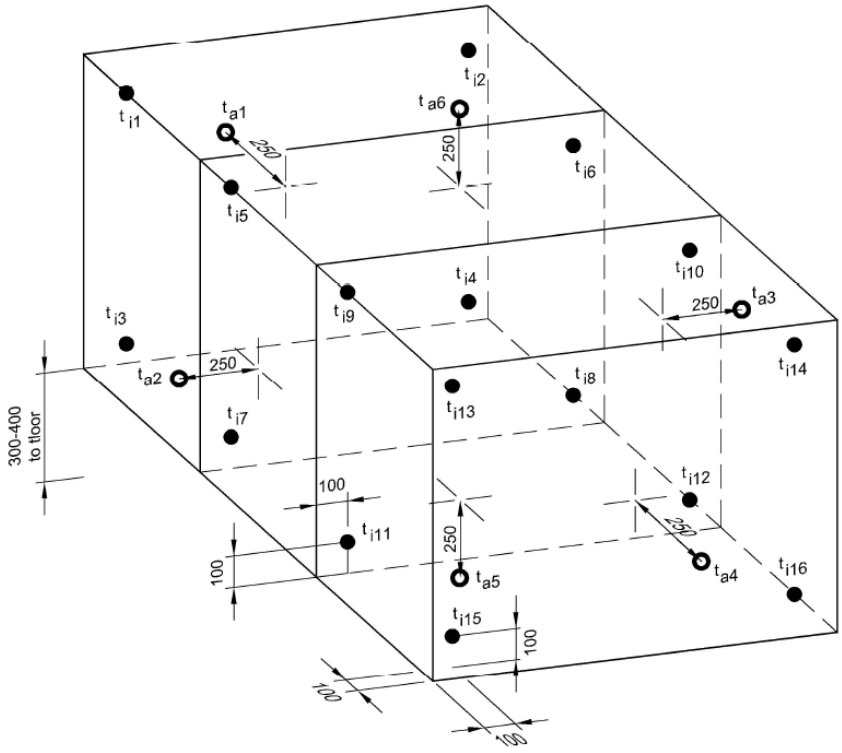


Figure 3.5 Installation of temperature sensors (EN 1886, 2007)



Figure 3.6 Front view of experimental setup

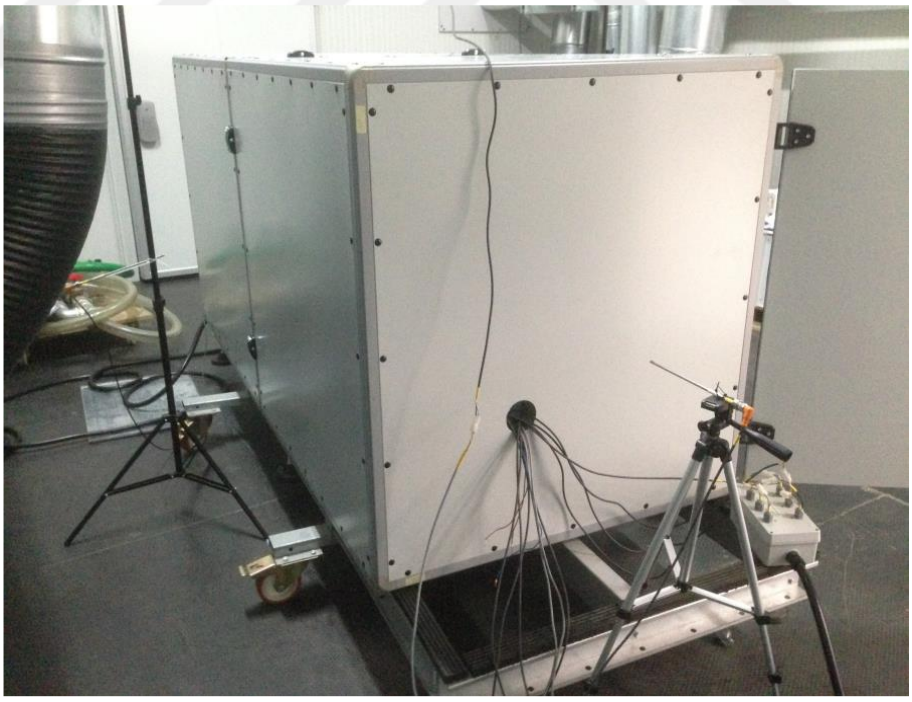


Figure 3.7 Back view of experimental setup

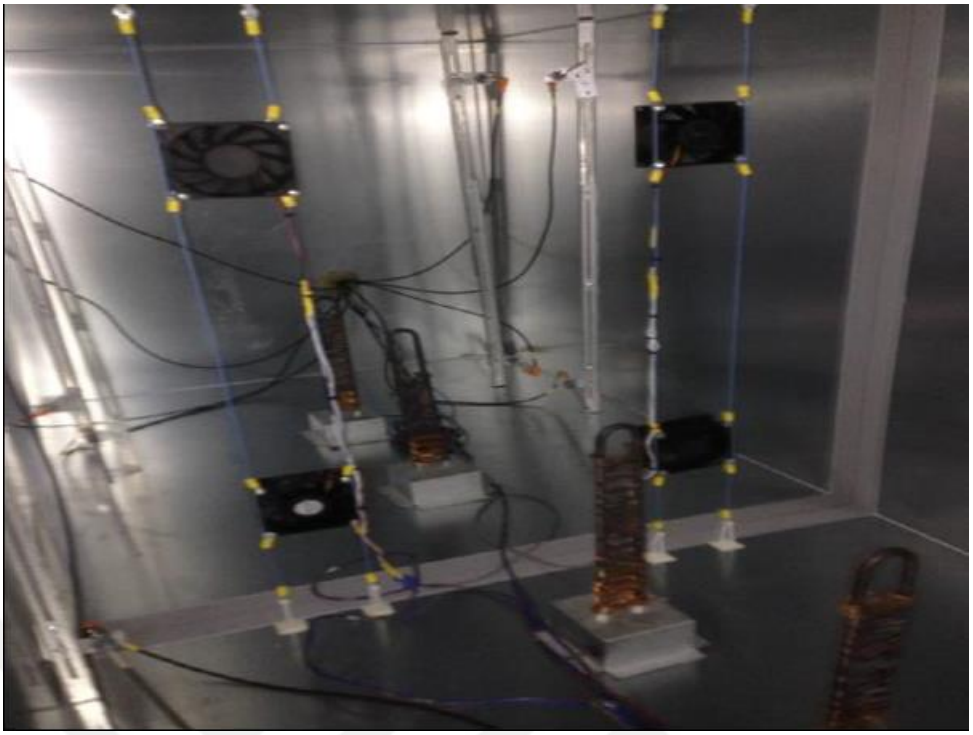


Figure 3.8 Location of fans and heating elements inside of the experimental setup

After test equipment is located, heaters and fans can be operated. Volumetric flow rate of air is calculated by using inner volume of the enclosure. Flow rate can be between 100 – 110 air change per hour. To obtain power of heaters to keep internal and external air temperature difference at 20˚C, heaters are controlled externally. Then during 30 minutes, standard deviation of the temperatures should not exceed 1.0 ˚C and for each zone, average air temperature difference can be maximum of 0.5 ˚C. If these conditions are met, temperature measuring can be started of external surface of the enclosure. By using the total power used by heaters and fans and maximum external surface temperature following values can be calculated;

1) Thermal Transmittance Class (T)
2) Thermal Bridging Class (TB)

These values can be affected by several parameters.

3.2.1.1 Thermal Transmittance

Thermal transmittance value U [W/m^{2}K] is calculated by using equation 3.1. In Table 3.1 thermal transmittance classifications can be seen.

$$U = \frac{P_{el}}{A \, x \, \Delta t_{air}} \tag{3.1}$$

where

P_{el} is the total electric power cosumed by heating elements and fans

A is total area of external surface

Δt_{air} is the air to air temperature difference

T_i is average temperature of internal air

T_a is average temperature of external air

Table 3.1 Thermal transmittance classes (EN 1886, 2007)

Class	Thermal Transmittance U [W/m^{2}K]
T1	$U \leq 0.5$
T2	$0.5 \leq U \leq 1$
T3	$1 \leq U \leq 1.4$
T4	$1.4 \leq U \leq 2$
T5	-

3.2.1.2 Thermal Bridging

Thermal bridging value k_b [-] is calculated by using equation 3.2. In Table 3.2 thermal bridging classifications can be seen.

$$k_b = \frac{\Delta T_{min}}{\Delta T_{air}} \tag{3.2}$$

where

ΔT_{min} is the least temperature difference, $\Delta T_{min} = T_i - T_{smax}$

ΔT_{air} is the air to air temperature difference, $\Delta T_{air} = T_i - T_a$

T_i is average temperature of internal air

T_a is average temperature of external air

T_{smax} is maxiumum measured outer surface temperature

Table 3.2 Thermal bridging classes (EN 1886, 2007)

Class	Thermal Bridging Factor k_b [-]
TB1	$0.75 \leq k_b \leq 1.00$
TB2	$0.60 \leq k_b \leq 0.75$
TB3	$0.45 \leq k_b \leq 0.60$
TB4	$0.30 \leq k_b \leq 0.45$
TB5	-

CHAPTER FOUR
NUMERICAL STUDY

4.1 Computational Fluid Dynamics (CFD)

4.1.1 Introduction to CFD

CFD is an engineering tool that helps to solve engineering problems related to heat and mass transfer, fluid dynamics. Fluid dynamics can be separated into two parts scientific and engineering. Scientific part investigates structure of heat and fluid flow and its physical phenomenon, such as boundary layer or separation of flow. This phenomenon can be obtained with using some physical inputs such as velocity, temperature, pressure or etc. Engineering part concentrates on certain parameters like lift force, drag force, pressure drop or rate of heat transfer (Sharma, 2021).

With the development of computers, engineering software became more popular. Commercial and open-source engineering programs were developed. Thus, engineering problems can be solved rapidly and more accurately.

4.1.2 The Fundamental equations of CFD

CFD software use fundament equations of fluid dynamics such as continuity, energy and momentum equations. The basic mathematical expressions of base physical phenomenon that science of fluid dynamics use these laws of conservation.

- The conservation of mass,
- The conservation of momentum,
- The conservation of energy.

There are three common solution methods that CFD codes use; finite element methods (FEM), finite difference methods (FDM), finite volume methods (FVM). In this study a CFD program was used that uses FVM. The schematic of control volume represented in Figure 4.1.

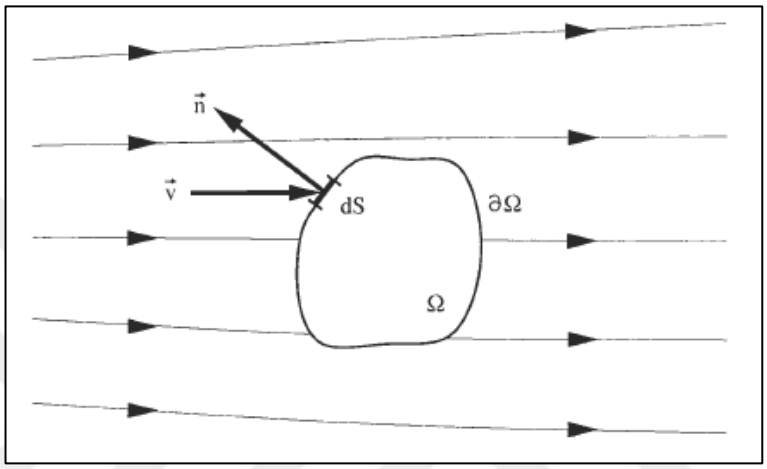


Figure 4.1 Schematic of control volume (Blazek, 2001)

4.1.3 Conservation Laws

4.1.3.1 The Continuity Equation

Using a finite control volume as seen in Figure 4.1, the continuity equation is derived. On the controls surface, the velocity of flow is represented with $\vec{v}$, the unit normal vector is $\vec{n}$ and *dS* represents minimum surface area. In this situation density (ρ) is the conserved quantity. To find total mass change per time of the finite volume **Ω**, there is

$$\frac{\partial}{\partial t}\int_{\Omega}\rho d\Omega \tag{4.1}$$

By the product of density, surface area and velocity component which is perpendicular to surface mass flow through surface of the fluid is calculated. Thus, the value comes from the convective flux across for every surface element dS becomes

$$\rho = (\vec{v}.\vec{n})dS \tag{4.2}$$

$\vec{n}$ always moves away from the control volume. According to sign of this value $(\vec{v}.\vec{n})$ flow direction can be determined. If the sign is negative, flow defined as inflow, otherwise flow defined as outflow.

$$\frac{\partial}{\partial t}\int_{\Omega} \rho d\Omega + \int_{\partial\Omega} \rho(\vec{v}.\vec{n})dS \tag{4.3}$$

With the integration of equation 4.3, integral form of the continuity equation can be calculated.

4.1.3.2 The Momentum Equation

To derive momentum equation, Newton's second law is used. Momentum occurs impact of the net force on the mass element. Control volume momentum **Ω**

$$\rho\vec{v}d\Omega \tag{4.4}$$

In the control volume change rate of momentum equals

$$\frac{\partial}{\partial t}\int_{\Omega} \rho\vec{v}d\Omega \tag{4.5}$$

The product of density times velocity is the conserved quantity.

$$\rho\vec{v} = [\rho u, \rho v, \rho w]^T \tag{4.6}$$

The convective flow tensors are defined by following components

$$\text{x-component} : \rho u \vec{v}$$

$$\text{y-component} : \rho v \vec{v}$$

$$\text{z-component} : \rho w \vec{v}$$

Convective flux tensor contributed to the conservation of momentum is calculated by

$$\iint_{\partial\Omega} \rho \vec{v}(\vec{v}.\vec{n}) dS \tag{4.7}$$

Two force types act on the control volume. Firs one is body forces which effects the mass of volume such as buoyancy, gravity. Second force is, come from directly surface of the control volume. Pressure distribution or shear and normal stresses can be given as an example.

Body (external) force effects on the conservation of momentum is

$$\int_{\Omega} \rho \vec{f_e} d\Omega \tag{4.8}$$

Isotropic pressure and viscous stress $\overline{\overline{\tau}}$ tensor composes surface sources.

$$\overline{\overline{Qs}} = -p\overline{\overline{I}} + \overline{\overline{\tau}} \tag{4.9}$$

In Figure 4.2, the surface sources are shown.

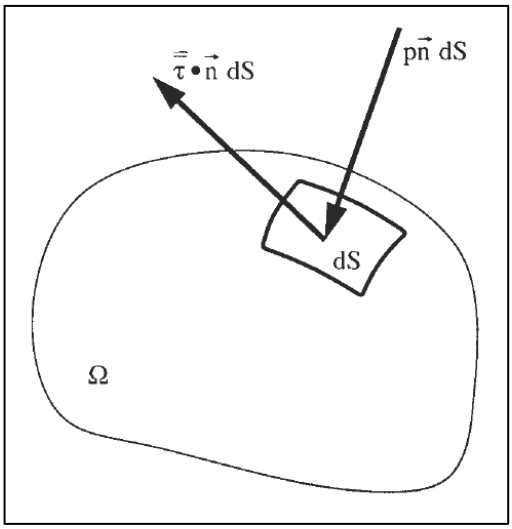


Figure 4.2 Forces have an impact on minimum surface dS (Blazek, 2001)

Equation 4.10 can be obtained with all equations were mentioned above.

$$\frac{\partial}{\partial t}\int_{\Omega}\rho\vec{v}d\Omega+\iint_{\partial\Omega}\rho\vec{v}(\vec{v}.\vec{n})dS=\int_{\Omega}\rho\vec{f}_{e}d\Omega-\iint_{\partial\Omega}p\vec{n}dS+\iint_{\partial\Omega}(\bar{\bar{\tau}}\vec{n})dS) \qquad (4.10)$$

Equation 4.10 expresses momentum conservation in a control volume.

4.1.3.3 The Energy Equation

Energy equation can be derived by using the first law of thermodynamics. Net heat flux and the rate of work of forces cause changes the total energy in the volume per time. Total energy can be calculated with adding the internal and kinetic energy per unit mass.

$$E=e+\frac{\left|\vec{v}\right|^{2}}{2}+\frac{u^{2}+v^{2}+w^{2}}{2} \qquad (4.11)$$

The conserved equation gives total energy per unit volume. The total energy variation in time is

$$\frac{\partial}{\partial t}\int_{\Omega}\rho E d\Omega \qquad (4.12)$$

The contribution of the convective flow can be expressed as

$$\oiint_{\partial\Omega} \rho E(\vec{v}.\vec{n})dS \tag{4.13}$$

In energy equation, there is diffusive flux which does not exist in continuity and momentum equations. Only internal energy is influential because of the diffusive flux $\overrightarrow{F_D}$ can be defined for the fluid at the state of rest.

$$\overrightarrow{F_D} = -\gamma\rho\kappa\nabla e \tag{4.14}$$

In Equation 4.14, $\gamma = \frac{c_p}{c_v}$ is the specific heat coefficient and κ is the thermal diffusivity coefficient. Equation 4.14 can be expressed as the Fourier law of heat conduction. In Equation 4.15, T represents the absolute static temperature and k represents the thermal conductivity.

$$\overrightarrow{F_D} = -k\nabla T \tag{4.15}$$

Net heat flux entering to the control volume can be effected by volumetric heating because of chemical reactions or radiation. Heat sources are represented - heat transfer per unit mass per time - as $\dot{q}_h$. The rate of work have been done by forces of body $\vec{f}$, that were used for the momentum equation, heat sources of volume were completed;

$$Q_v = \rho\vec{f}\vec{v} + \dot{q}_h \tag{4.16}$$

$\vec{Q}_s$ is the final parameter affected by the energy conservation law.

This conform with the work done per time by the pressure on the fluid element;

$$\vec{Q}_s = -p\vec{v} + \vec{\vec{\tau}}\vec{v} \tag{4.17}$$

With using equations above, conservation of energy can be stated as;

$$\frac{\partial}{\partial t}\int_{\Omega} \rho E d\Omega + \oiint_{\partial\Omega} \rho E(\vec{v}\vec{n})dS = \oiint_{\partial\Omega} k(\nabla T\vec{n})dS + \int_{\Omega} (\rho \overrightarrow{f_e}\vec{v} + \dot{q}_h)d\Omega - \oiint_{\partial\Omega} p(\vec{v}\vec{n})dS + \oiint_{\partial\Omega} (\vec{\vec{\tau}}\vec{v})\vec{n}dS \tag{4.18}$$

4.2 Numerical Study

Manufacturing a prototype to observe positive and negative effects of each new design parameter, can be ineffective way in terms of time and cost. To eliminate disadvantages of manufacturing a prototype, engineering simulation software can be used. In this first step of the numerical study, a numerical model was created which have same material properties and dimensions with the model that used in experimental study. After numerical model was validated with experimental results, new panel sections with different thicknesses were modeled and analyzed.

4.2.1 CFD Model

Figure 4.3 and Figure 4.4 shows internal and external edges of prototype. In table 4.1 dimensions of this edges can be seen.

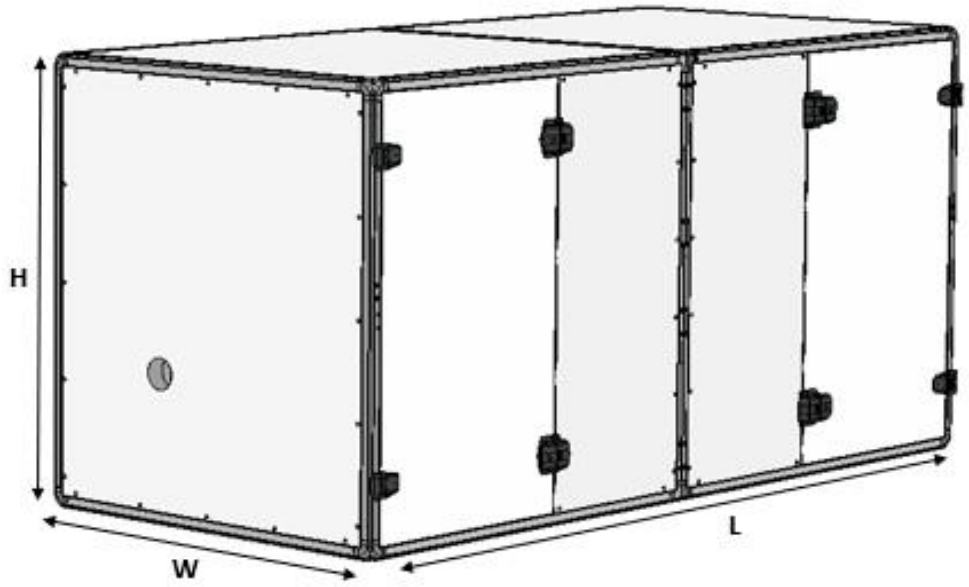


Figure 4.3 External dimensions of prototype

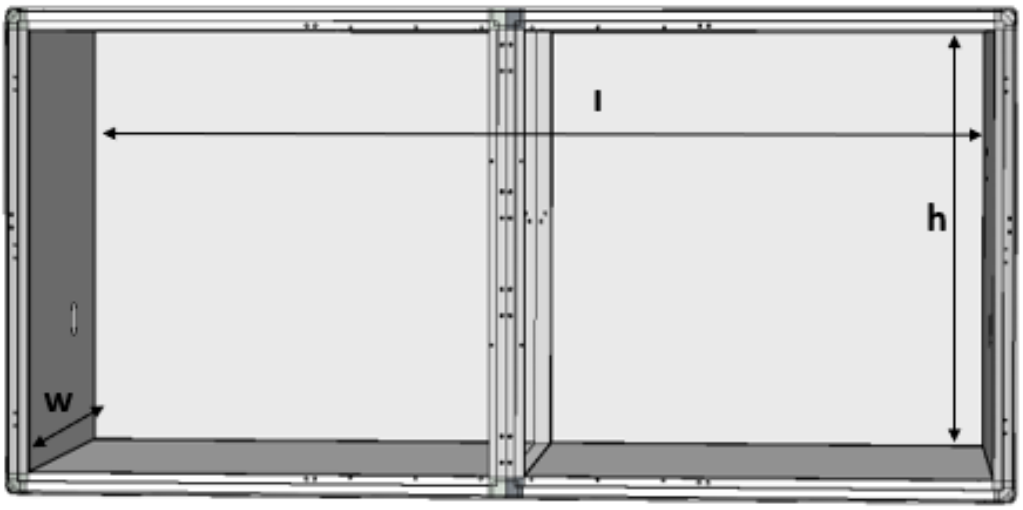


Figure 4.4 Internal dimensions of prototype

Table 4.1 Dimensions of prototype

H	1126 mm
L	2326 mm
W	1057 mm
h	1026.4 mm
l	2226.4 mm
w	957.4 mm

In Figure 4.5, section details of panel which has 50 mm of thickness and in Table 4.2, thermal conductivity of materials can be seen.

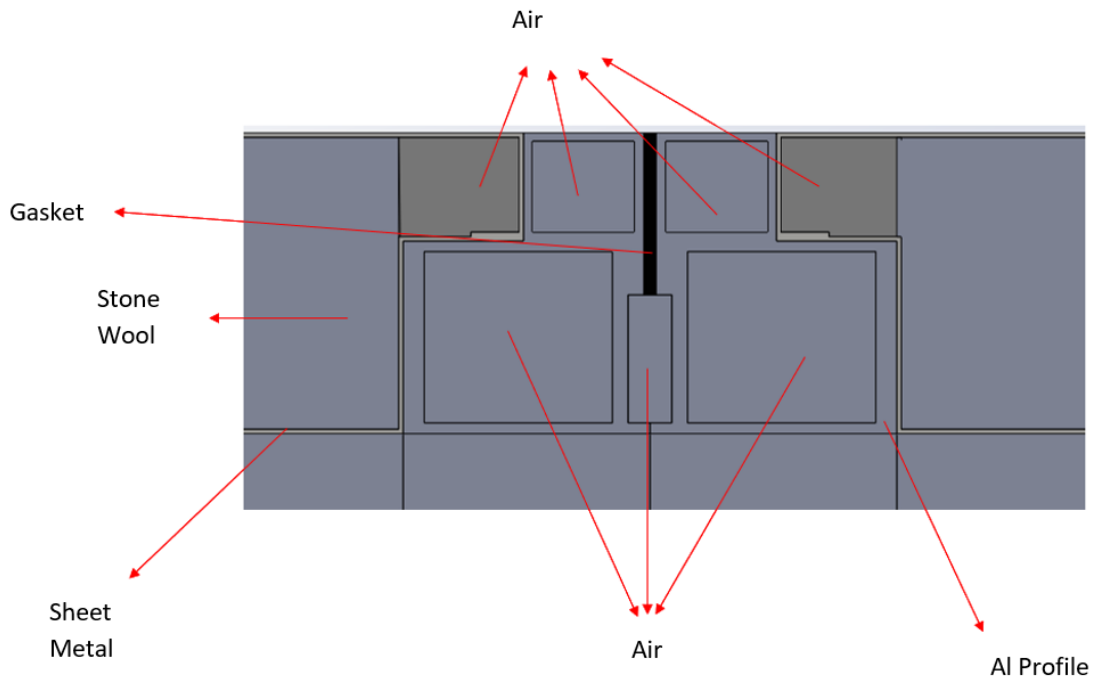


Figure 4.5 View of panel section

Table 4.2 Thermal conductivity of materials

Material	**Thermal conductivity [W/m. K]**
Al Profile 6060 T6	210
Sheet metal	16
Gasket	0.180
Stone wool	0.036

4.2.2 Meshing

Mesh number is one of the most important parameters for more reliable results in CFD software. Although much mesh number means more reliable results, there should be limit on mesh numbers because of the limits of computers. To find optimum number of mesh, mesh independence study was done. Change of the average and maximum temperature on the top surface with increasing number of elements can be seen in Table 4.3.

Table 4.3 Mesh independence study

Number of elements	**Temperature on the top surface point [˚C]**	**Average temperature on top surface [˚C]**
293086	29.733	23.87
358075	30.02	23.56
570943	31.058	24.77
850555	31.098	24.93
988271	31.072	24.89

According to mesh independence study results, Figure 4.6 and 4.7 shows that change of the temperature for different number of mesh.

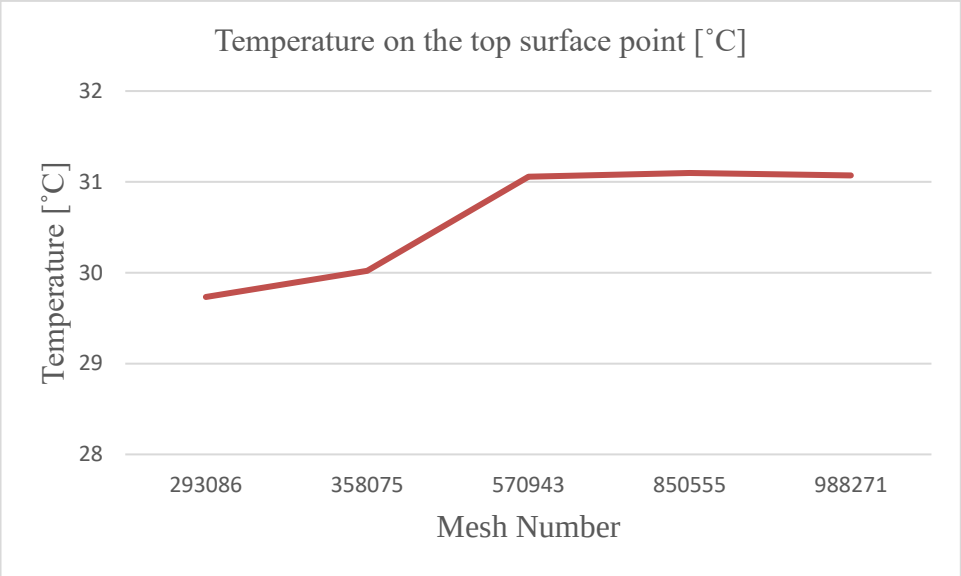


Figure 4.6 Maximum top surface temperature for more number of elements

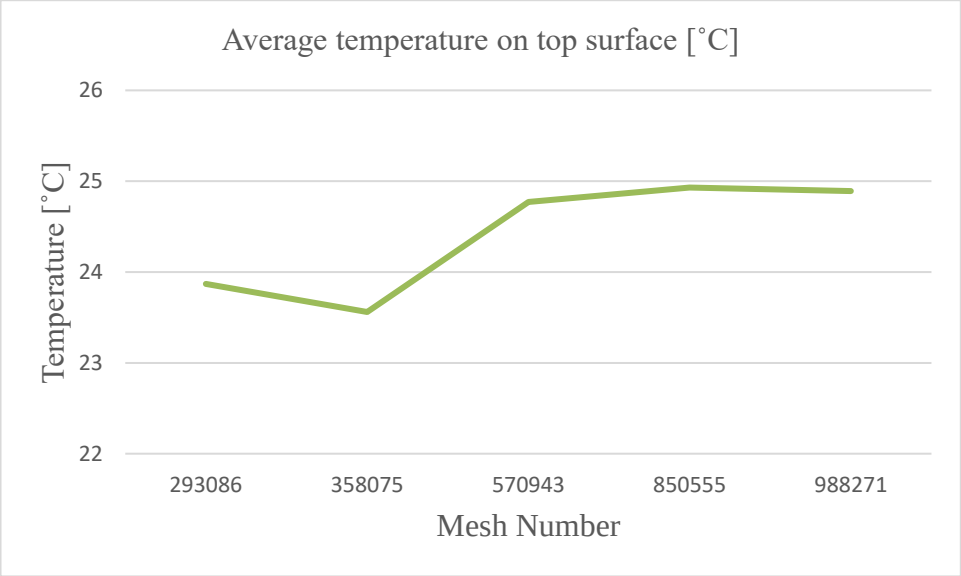


Figure 4.7 Average top surface temperature for more number of elements

Optimum node and element numbers which is found by doing mesh independence study is shown in Table 4.4.

Table 4.4 Node and element numbers

Number of node	153704
Number of elements	570943

Mesh quality for the model which have optimum element number was also examined. Optimum element number is 570943 and average element quality is 0.76. In Figure 4.8 mesh structure of the model for optimum element number is shown.

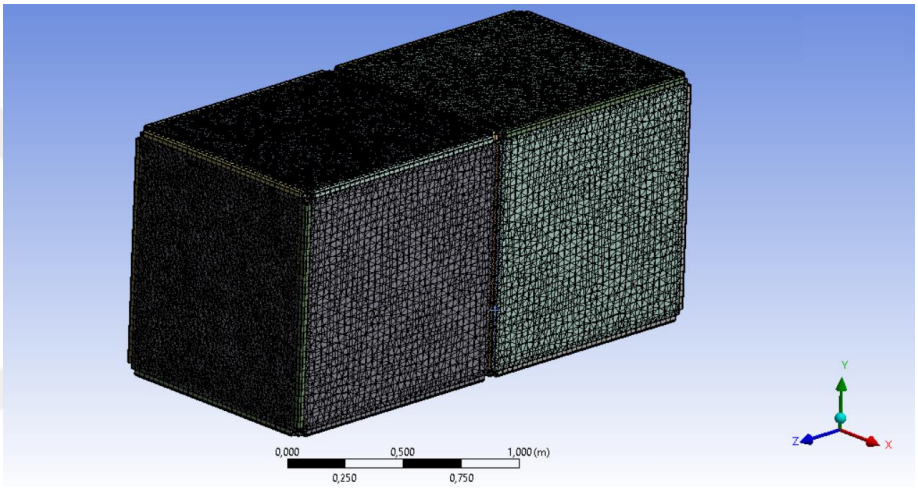


Figure 4.8 Mesh structure of CFD model

4.2.3 Boundary Conditions

Still air convective heat transfer coefficient data embedded in commercial CFD software was used for external air convective heat transfer coefficient. Due to internal air has forced convection, internal air convective heat transfer coefficient is bigger. These convective heat transfer coefficients and experimental data used for internal and external air temperatures as boundary conditions are shown in Table 4.5.

Table 4.5 Boundary conditions

Internal air temperature (˚C)	37.1
Exterrnal air temperature (˚C)	17.1
External air convective heat transfer coefficient (W/m2. K)	2.25
Internal air convective heat transfer coefficient (W/m2. K)	6

CHAPTER FIVE
RESULTS AND DISCUSSIONS

5.1 Experimental Results

After the conditions met as mentioned in chapter 3.2.1, temperature measuring was made on the external surface of prototype. The point of maximum surface temperature (T_{smax}) is shown in Figure 5.1

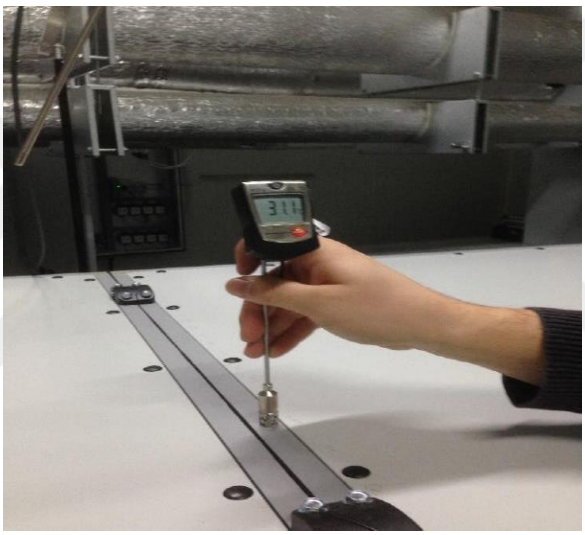


Figure 5.1 Location of the maximum surface temperature

Figure 5.2 and Figure 5.3 shows that the results of front and top surface temperature measurings.

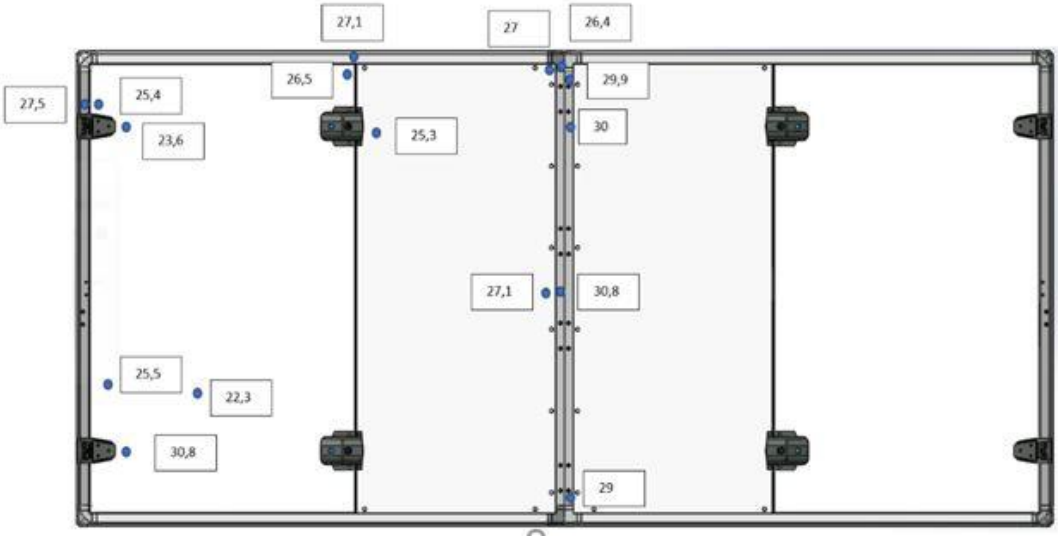


Figure 5.2 Front side temperature measuring results

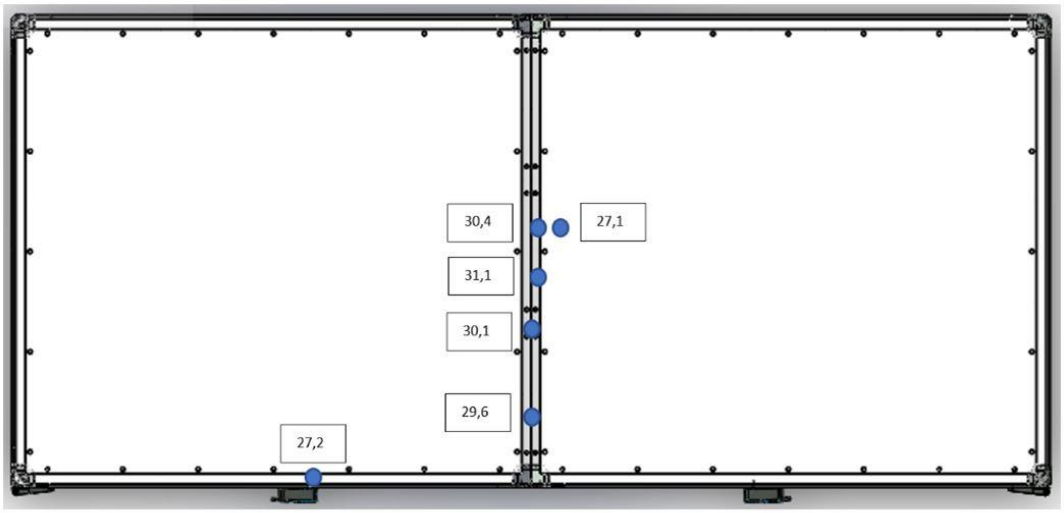


Figure 5.3 Top surface temperature measuring results

In Table 5.1 shows that experimental measuring results and calculations according to chapter 3.2.1.1 and chapter 3.2.1.2.

Table 5.1 Experimental data

Average temperature of internal air - T_i [°C]	37.13
Average temperature of external air - T_a [°C]	17.11
ΔT_{air} [°C]	20.02
T_{smax} [°C]	31.10
External surface area [m^2]	12.54
$P_{heaters}$ [W]	315
P_{fan} [W]	26.70
P_{el} [W]	341.70
U [$W/m^2.K$]	1.36
k_b [-]	0.30

5.2 Numerical Results

Figure 5.4 shows that the results of front and top surface temperature of the CFD analysis. Comparison of the experimental and numerical results are given in Table 5.2.

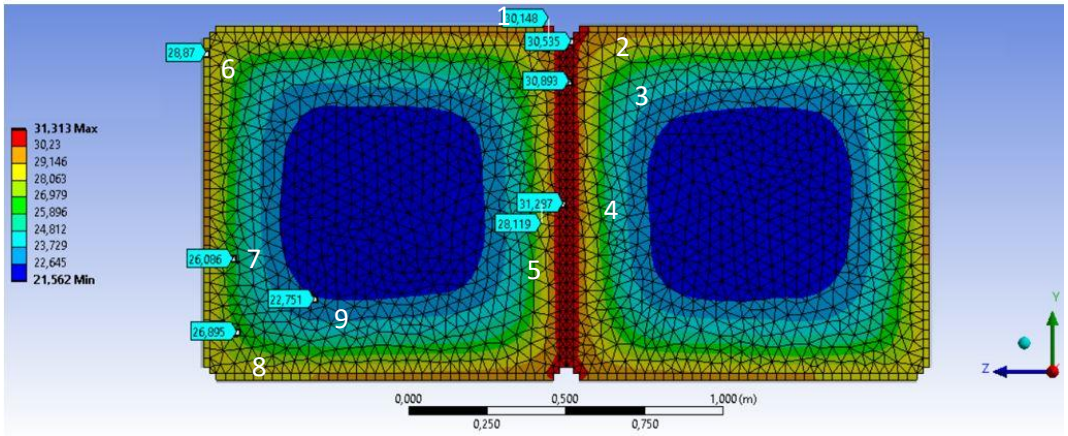


Figure 5.4 Numerical study results of front view

Table 5.2 Comparison of experimental and numerical results of front view

Measuring Point	Numerical Results [˚C]	Experimental Results [˚C]	Error margin [%]
1	30.148	27	-11.66
2	30.535	29.9	-2.12
3	30.893	30	-2.98
4	31.287	30.8	-1.58
5	28.119	27.1	-3.76
6	28.87	27.5	-4.98
7	26.086	25.5	-2.30
8	26.895	30.8	12.68
9	22.751	22.3	-2.02

Figure 5.5 shows that the results of front and top surface temperature of the CFD analysis. Comparison of the experimental and numerical results are given in Table 5.3.

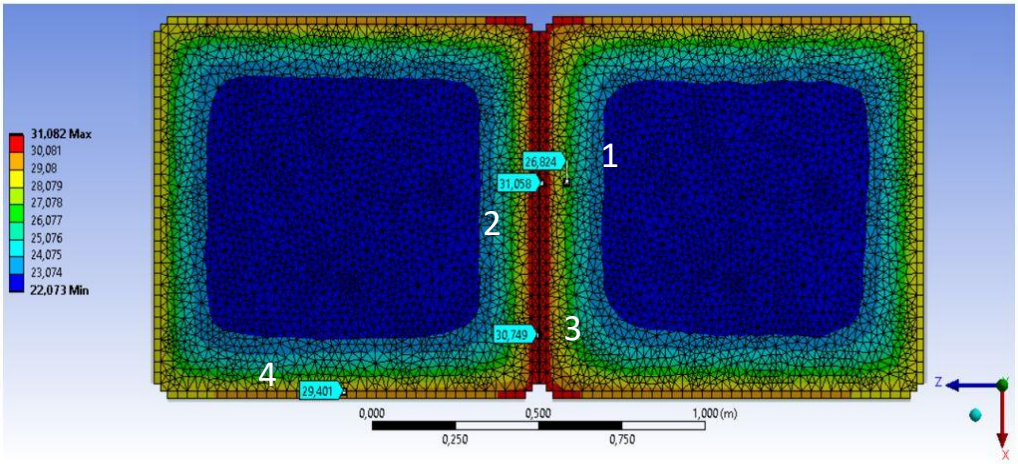


Figure 5.5 Numerical study results of top view

Table 5.3 Comparison of experimental and numerical results of top view

Measuring Point	Numerical Results [˚C]	Experimental Results [˚C]	Error margin [%]
1	31.058	31.1	0.14
2	26.824	27.1	1.02
3	30.749	29.6	-3.88
4	29.401	27.02	-8.81

After numerical studies validated with experimental data for 50 mm panel thickness model, new numerical models were prepared with 55 and 60 mm panel thicknesses. In Figure 5.6 and Figure 5.7, top view temperature results can be seen for the 55 and 60 mm panel thickness models, respectively.

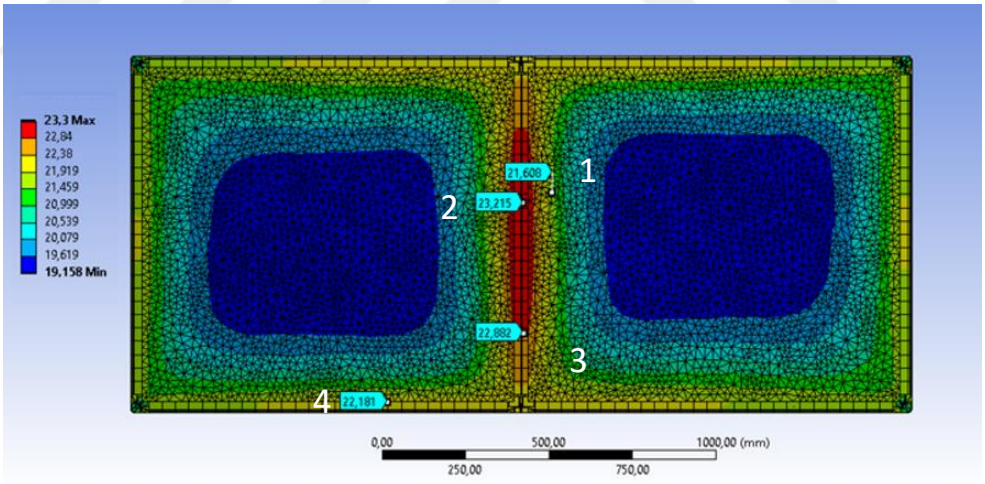


Figure 5.6 Temperature measuring results of top view of 55 mm panel thickness model

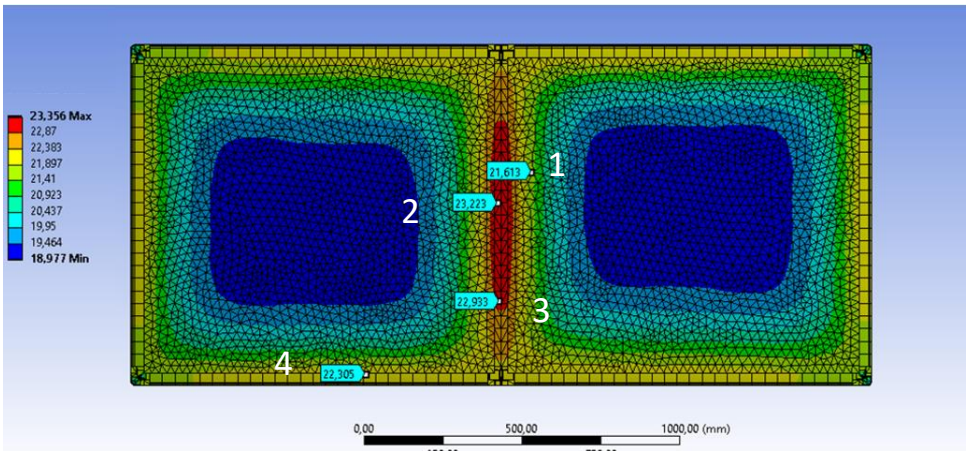


Figure 5.7 Temperature measuring results of top view of 60 mm panel thickness model

The temperature results for top view of models which have obtained with numerical study can be seen in Table 5.4.

Table 5.4 Comparison of the temperature results of top view of models

Measuring Point	**Panel Thickness [mm]**					
	50		**55**		**60**	
	Temp. [˚C]	**Thermal Bridging**	**Temp. [˚C]**	**Thermal Bridging**	**Temp. [˚C]**	**Thermal Bridging**
1	31.058	TB4 (k_b=0.302)	21.608	TB2 (k_b=0.694)	21.613	TB2 (k_b=0.693)
2	26.824		23.215		23.223	
3	30.749		22.882		22.933	
4	29.401		22.181		22.305	

CHAPTER SIX
CONCLUSIONS

In this study, heat insulation performance of a ventilation unit casing was investigated by conducting experimental and numerical studies. Experimental study carried out according to EN 1886 “Ventilation for buildings - Air handling units - Mechanical performance ” standard. A prototype was provided by the manufacterer and experiments were completed in manufacturer’s site. Panels with 50 mm thickness have been used for prototype. In numerical study, prototype was modeled on CAD software with same physical properties and dimensions. CAD model imported to commercial CFD software and CFD analysis have been completed. Experimental data was used as boundary conditions in numerical model. Results of the analysis widely agreed with experimental results. Especially critical points which measured maximum surface temperatures have error margin up to 2%. Some points which have lower temperature measurings have 12% difference between experimental and numerical results. These percentages are in acceptable range when literature examined. After the numerical model was verified with experimental data, effects of panel thickness on thermal performance were investigated by doing numerical analysis.

As a result of the study, the panel thickness was increased from 50 mm to 55 mm, the maximum temperature measured on the external surface of the casing decreased by approximately 10˚C. If the results will be compared in terms of EN 1886 Standard classification range, as can be seen in Table 5.4, thermal bridging class enhanced from TB4 to TB2 for 55 and 60 mm panel thickness models. However, a significant performance increase was not observed in the model with 60 mm panel thickness compared to the 55 mm model. It was concluded that the optimum panel thickness is 55 mm, as the effect of increasing the section thickness is very small.

REFERENCES

American Society of Heating, Refrigerating and Air-Conditioning Engineers (ASHRAE) Terminology. (2021, December 20). *Definition of air handling unit*. https://xp20.ashrae.org/terminology/index.php?term=handling&submit=Search

Asdrubali, F., Baldinelli, G. & Bianchi, F. (2011). A quantitative methodology to evaluate thermal bridges in buildings. *Applied Energy, 97*, 365-373.

Baba, F. & Ge, H. (2016). Dynamic effect of balcony thermal bridges on the energy performance of a high-rise residential buildings in Canada. *Energy And Buildings, 116*, 78-88.

Beşer, E., Mobedi, M. & Kumlutaş, D. (2001). Klima santral kesitlerinin ısıl özellikleri. *5. Ulusal Tesisat Mühendisliği Kongresi,* İzmir.

Blasinski, P., Rubina, A., Rubinova, O., & Juza, S. (2021). Adaptive fan control. *3rd International Conference On The Sustainable Energy And Environmental Development,* Krakow.

Blazek, J. (2001). *Computational fluid dynamics: Principles and applications* (1st ed.). Netherlands: Elsevier Science Ltd.

Brumbaugh, J., E. (2004). *Hvac fundamentals volume 1: heating systems, furnaces and boilers* (4th ed.). USA: Wiley Publishing.

Çengel, Y., A. (2002). *Heat transfer - a practical approach* (2nd ed.). USA: McGraw – Hill.

Directive 2005/32/EC of the European Parliament and of the Council of 6 July 2005. Establishing a framework for the setting of ecodesign requirements for energy-using products. *Official Journal of the European Union*, 191, 29-58.

EN 1886 Ventilation for buildings – Air handling units – Mechanical performance English version of DIN EN 1886:2007.

Etheridge, D. (2012). *Natural ventilation of buildings: Theory, measurement and design* (1st ed.). USA: John Wiley & Sons Ltd.

Gulmez, M. & Yilmaz, D. (2020). Design and development of refrigerator door gasket to prevent condensation. *Heat Ttransfer And Research, 51,* 1061-1072.

Kalbasi, R., Shahsavar, A. & Afrand, M. (2019). Reducing AHU energy consumption by a new layout of using heat recovery units. *Journal Of Thermal Analysis And Calorimetry, 139,* 2811-2820.

Korkmaz, B. (2013). *Numerical and experimental investigations of heat transfer in a cross – flow heat recovery system.* M. Sc. Thesis, Dokuz Eylül University, İzmir.

Kwon, S., B., Kim, S., Park, D., S., Cho, Y., Kim, J., Kim, M. & Kim, T. (2011). Novel air filtration device for building air handling unit. *Aeorosol And Air Quality Research, 11,* 570-577.

Lei, L., Bortolin, A., Bison, P. & Maldague, X. (2017). Detection of insulation flaws thermal bridges in insulated truck box panels. *Quantitative Infrared Thermography Journal,* 14, 275-284.

Liu, M., Claridge, D., E., Deng, S. (2003). An air filter pressure loss model for fan energy calculation in air handling units. *International Journal Of Energy Research, 27,* 598-600.

Martin, K., Campos-Celador, A., Escudero, C., Gomez, I & Sala, J.M (2012). Analysis of thermal bridge in a guarded hot box testing facility. *Energy And Buildings, 50,* 139-149.

Mcdowall, R. (2006). *Fundamentals of hvac systems* (1th ed.). USA: Elsevier.

Navarro, H., A., Gomez, L., C. (2005). A new approach for thermal performance calculation of cross – flow heat exchangers. *Internal Journal Of Heat And Mass Transfer, 48,* 3880-3888.

Oughton, D., R. & Hodkinson, S., L. (2008). *Faber and kell's heating and air conditioning of buildings* (10th ed.). USA: Elsevier.

Pospisil, T., Pencik, J., Matejka, L., Kaluzova, A. & Dostalova, D. (2012). Elimination of thermal bridge by thermal insulation composite material. *Advanced Materials Research, 482-484,* 1654-1659.

Promoppatum, P., Yao, S., C., Hultz, T. & Agee, D. (2017). Experimental and numerical investigation of the cross – flow pcm heat exchanger for the energy saving of building hvac. *Energy And Buildings 138,* 468-478.

Seara J., F., Diz, R., Uhia, F., J., Dopazo, A. & Ferro, J., M. (2010). Experimental analysis of an air to air heat recovery unit for balanced ventilation systems in residential buildings. *Energy Conversion And Management, 52,* 635-640.

Sharma, A. (2021). *Introduction to computational fluid dynamics* (1th ed.). Switzerland: Springer.

Söylemez, M., S. (2007). Optimum length of finned pipe for waste heat recovery. *Energy Conversion And Management, 49,* 96-100.

Tadeu, A., Simoes, I., Simoes, N. & Prata, J. (2011). Simulation of dynamic linear thermal bridges using a boundary element method model in the frequency domain. *Energy And Buildings, 43,* 3685-3695.

Thiessen, S., Knabben, F., T., Melo, C. & Gonçalves, J., M. (2018). A study on the effectiveness of applying vacuum insulation panels in domestic refrigerators. *Internal Journal Of Refrigeration, 96,* 10-16.

Thulukkanam, K. (2013). *Heat exchanger design book* (2th ed.). USA: CRC Press.

Tian, E. & Mo, J. (2019). Toward energy saving and high efficency through an optimized a PET coarse filter: The development of a new electrostatically assisted air filter. *Energy & Buildings, 186,* 276-283.

Yang, F., Yuan, X. & Lin, G. (2003). Waste heat recovery using heat pipe heat exchanger for heating automobile using exhaustgas. *Applied Thermal Engineering, 23*. 367-372.

Zenginoğlu, M., Koçak, M. & Salman, İ., M. (2019). Klima santrallerinde ısı köprüsü oluşumunun deneysel ve sayısal olarak incelenmesi. *14. Ulusal Tesisat Mühendisliği Kongresi,* İzmir.

Wallin, J., Madani, H. & Claesson, J. (2012). Run-around coil ventilation heat recovery system: A comparative study between different system configurations. *Applied Energy, 90*, 258-265.